

AD No. 408779

ASD-TDR-62-984

408 779

63 4-2

DDC FILE COPY

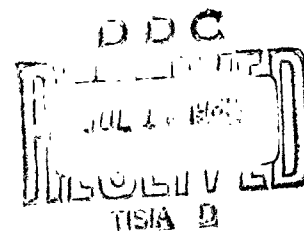
## RECOVERY BEHAVIOR OF COLD-WORKED METALS

TECHNICAL DOCUMENTARY REPORT NO. ASD-TDR-62-984

May 1963

Directorate of Materials and Processes  
Aeronautical Systems Division  
Air Force Systems Command  
Wright-Patterson Air Force Base, Ohio

Project No. 7351, Task No. 735106



(Prepared Under Contract No. AF 33(616)-8346 by Lockheed Missiles & Space  
Company, Sunnyvale, California,  
J. L. Lytton, T. E. Tietz, C. L. Meyers, authors)

## NOTICES

When Government drawings, specifications, or other data are used for any purpose other than in connection with a definitely related Government procurement operation, the United States Government thereby incurs no responsibility nor any obligation whatsoever; and the fact that the Government may have formulated, furnished, or in any way supplied the said drawings, specifications, or other data, is not to be regarded by implication or otherwise as in any manner licensing the holder or any other person or corporation, or conveying any rights or permission to manufacture, use, or sell any patented invention that may in any way be related thereto.

Qualified requesters may obtain copies of this report from the Armed Services Technical Information Agency, (ASTIA), Arlington Hall Station, Arlington 12, Virginia.

This report has been released to the Office of Technical Services, U.S. Department of Commerce, Washington 25, D.C., in stock quantities for sale to the general public.

Copies of this report should not be returned to the Aeronautical Systems Division unless return is required by security considerations, contractual obligations, or notice on a specific document.

B

## FOREWORD

This report was prepared by the Lockheed Missiles & Space Company under USAF Contract No. AF 33(616)-8346. This contract was initiated under Project No. 7351, "Metallic Materials," Task No. 735106, "Behavior of Metals." The project was administered by the Directorate of Materials and Processes, Deputy for Technology, Aeronautical Systems Division, with Lt. C. S. Cook acting as Project Engineer.

This report covers work conducted from 1 June 1961 to 31 August 1962.

This report was prepared as Technical Report No. 2-90-62-1 by T. E. Tietz, J. L. Lytton, and C. L. Meyers, scientists in the Materials Sciences Laboratory at LMSC. Acknowledgment is made to L. C. Potter for assistance during this program.

## ABSTRACT

Recovery of tensile flow stress of four binary aluminum alloys and of the high-purity base aluminum was studied under no-load conditions at temperatures of 80°, 120°, 160°, and 200°C, and under conditions of creep strain at 160°C, for recovery times up to 1,000 hr.

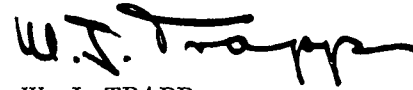
At the three higher recovery temperatures, 120°, 160°, and 200°C, and for the longer recovery times, the alloys Al-Mg, Al-Zn, and Al-Cu all experienced a greater degree of recovery than the high-purity base aluminum. Of these three alloys, the Al-Cu alloy clearly exhibited the greatest degree of recovery. The Al-Ag alloy was excluded from the comparison because of an apparent strengthening process which occurred during recovery.

All the alloys showed a strong increase in flow-stress recovery during creep strain over that experienced during no-load recovery; however, the relative order of recovery for the different alloys did not change.

The recovery of flow stress of recrystallized arc-cast molybdenum after 10% prestrain at 150°C was studied for recovery temperatures of 725°, 801°, and 901°C. The yield phenomenon observed after recovery was such that the yield drop diminished and disappeared as recovery proceeded. A fractional flow-stress recovery parameter  $f_r$  was developed and it was shown that, independent of recovery temperature, equal  $f_r$  values of about 0.16 produced superposition of stress-strain curves except for the initial yield phenomenon. The activation energy for low degrees of recovery was found to be 32,600 calories per mole in close agreement with a reported value for diffusion of carbon in molybdenum. Above an  $f_r$  value of about 0.15 where recovery was thought to predominate over strain-aging, the activation energy varied from 43,600 to 82,500 calories per mole and increased with increasing recovery and recovery temperature.

A 10% prestrain shifted the ductile-brittle transition temperature, as indicated by tensile elongation, from 10° C to about - 22° C. A 100-hr recovery anneal at 801° C was shown to shift the transition temperature to about - 5° C, the major shift occurring during the first hour of recovery.

This technical documentary report has been reviewed and is approved.

A handwritten signature in black ink, appearing to read 'W. J. Trapp', with a stylized, cursive script.

W. J. TRAPP  
Chief, Strength and Dynamics Branch  
Metals and Ceramics Laboratory  
Directorate of Materials and Processes

## TABLE OF CONTENTS

Section		Page
	Part I: RECOVERY OF ALUMINUM AS INFLUENCED BY DILUTE SOLID-SOLUTION ADDITIONS OF MAG- NESIUM, ZINC, COPPER, AND SILVER	
1	INTRODUCTION	1
2	EXPERIMENTAL PROCEDURE	3
	2.1 Test Materials	3
	2.2 Apparatus	5
	2.3 Method of Evaluating Recovery	10
3	EXPERIMENTAL RESULTS	13
	3.1 Recovery Behavior of the High-Purity Base Aluminum	13
	3.2 Recovery Behavior of the Aluminum Alloys	15
	3.3 Recovery Behavior of the High-Purity Aluminum and the Four Binary Alloys Under Conditions of Concurrent Plastic Strain	26
4	SUMMARY	33
	Part II: RECOVERY BEHAVIOR OF UNALLOYED ARC-CAST MOLYBDENUM	
5	INTRODUCTION	35
6	EXPERIMENTAL PROCEDURE	37
	6.1 Test Materials	37
	6.2 Apparatus	38
	6.3 Method of Evaluating Flow-Stress Recovery	42

TABLE OF CONTENTS (CONT'D)

Section		Page
7	EXPERIMENTAL RESULTS	47
	7.1 Stress-Strain Results	47
	7.2 Flow-Stress Recovery of Arc-Cast Molybdenum	49
	7.3 Effect of Recovery on the Ductility of Arc-Cast Molybdenum	56
8	DISCUSSION	59
	8.1 Strain-Aging Effects	59
	8.2 Flow-Stress Recovery	60
9	SUMMARY	63
	REFERENCES	65

## LIST OF ILLUSTRATIONS

Figure		Page
1	Tensile Test Specimen Design	4
2	Tensile Specimen and Extensometer Assembly in Test Position	7
3	Constant Temperature Baths Used for Recovery Under No-Load Conditions	8
4	Experimental Setup for Studying Recovery Behavior Under Conditions of Concurrent Stress	9
5	Schematic Diagram Showing the Effect of Recovery on the Stress-Strain Curve and the Method Used To Evaluate the Degree of Recovery	11
6	Fractional Recovery as a Function of Recovery Time for 99.99 <sup>+</sup> % Aluminum at Four Recovery Temperatures	14
7	Fractional Recovery as a Function of Recovery Time for Al-0.1% Mg Alloy at Four Recovery Temperatures	16
8	Fractional Recovery as a Function of Recovery Time for Al-0.1% Cu Alloy at Four Recovery Temperatures	16
9	Fractional Recovery as a Function of Recovery Time for Al-0.1% Zn Alloy at Four Recovery Temperatures	18
10	Fractional Recovery as a Function of Recovery Time for Al-0.1% Ag Alloy at Four Recovery Temperatures	18
11	Fractional Recovery Versus Recovery Time for Aluminum and the Four Binary Aluminum Alloys at 80°C	19
12	Fractional Recovery Versus Recovery Time for Aluminum and the Four Binary Aluminum Alloys at 120°C	19
13	Fractional Recovery Versus Recovery Time for Aluminum and the Four Binary Aluminum Alloys at 160°C	20
14	Fractional Recovery Versus Recovery Time for Aluminum and the Four Binary Aluminum Alloys at 200°C	20
15	True Stress - True Strain Curves for Aluminum and the Four Binary Alloys at 160°C	23
16	Decrease in Room-Temperature Flow Stress During Recovery at 160°C for Aluminum and Three Binary Aluminum Alloys	25



# LIST OF ILLUSTRATIONS (CONT'D)

Figure		Page
17	Initial Flow Stress After Recovery as a Function of Recovery Time at 160° C for Aluminum and Three Binary Aluminum Alloys	25
18	Effect of Creep Strain at a Stress of 1,900 psi on the Recovery of 99.99+% Aluminum at 160° C	27
19	Effect of Creep Strain at a Stress of 1,900 psi on the Recovery of the Al-0.1% Mg Alloy at 160° C	28
20	Effect of Creep Strain at a Stress of 1,900 psi on the Recovery of the Al-0.1% Cu Alloy at 160° C	28
21	Effect of Creep Strain at a Stress of 1,900 psi on the Recovery of the Al-0.1% Zn Alloy at 160° C	29
22	Effect of Creep Strain at a Stress of 1,900 psi on the Recovery of the Al-0.1% Ag Alloy at 160° C	29
23	Total Fractional Recovery During Creep Strain at a Stress of 1,900 psi for Aluminum and the Four Binary Alloys at 160° C	31
24	Increase in Fractional Recovery Due to Creep as a Function of Creep Strain for Aluminum and the Four Binary Aluminum Alloys Under a Stress of 1,900 psi at 160° C	31
25	Molybdenum Tensile Test Specimen Design	39
26	Schematic View of Stainless Steel Can and Quartz Capsule Assembly	41
27	Schematic Diagram Showing the Method Used To Evaluate the Degree of Recovery of Arc-Cast Molybdenum	43
28	Effect of Room-Temperature Aging on the Flow Stress at 10% Strain of Recrystallized Arc-Cast Molybdenum	45
29	Stress-Strain Curves for Recrystallized Arc-Cast Molybdenum Showing Various Lower Yield Effects	48
30	Schematic Illustration of the Joining of Two Lüders Bands During Tensile Straining of Arc-Cast Molybdenum	50
31	Effect of Recovery Time at 725° C After 10% Prestrain on the Flow Behavior of Recrystallized Arc-Cast Molybdenum	52
32	Effect of Recovery Time at 801° C After 10% Prestrain on the Flow Behavior of Recrystallized Arc-Cast Molybdenum	52
33	Effect of Recovery Time at 901° C After 10% Prestrain on the Flow Behavior of Recrystallized Arc-Cast Molybdenum	53
34	Effect of Recovery Time on the Fractional Flow-Stress Recovery of Recrystallized Arc-Cast Molybdenum for Three Recovery Temperatures	54

# LIST OF ILLUSTRATIONS (CONT'D)

Figure		Page
35	Stress-Strain Curves for Three Arc-Cast Molybdenum Specimens With Equal Values of Fractional Flow-Stress Recovery	55
36	Effect of Prestrain and Recovery Treatment on the Elongation to Fracture of Recrystallized Arc-Cast Molybdenum	57
37	Effect of Melting Temperature on the Activation Energy for Flow-Stress Recovery of Metals	62

# LIST OF TABLES

Table		
1	Chemical Analyses of Test Materials	3
2	Room-Temperature of Solid Solubility Data and Change in Lattice Parameter of Aluminum per Atomic Percent Solute	5
3	Recrystallization Treatment	5
4	Processing Schedule for Arc-Cast Molybdenum	37

Part I

RECOVERY OF ALUMINUM AS INFLUENCED BY DILUTE SOLID-SOLUTION  
ADDITIONS OF MAGNESIUM, ZINC, COPPER, AND SILVER

T. E. Tietz

C. L. Meyers

## Section 1

### INTRODUCTION

An initial study was conducted in the Materials Sciences Laboratory of Lockheed Missiles & Space Company for the Aeronautical Systems Division under contract AF 33(616)-7156. The results of this study were reported in detail in the final technical report, WADD TR 61-138, dated February 1961. Based upon the first year's work, two papers were accepted for publication. (1, 2)

In the initial study, the effect of elastic strain, plastic strain, and a 1% magnesium addition on the recovery behavior of a high-purity base aluminum was investigated. The degree of recovery of the prestrained test material was measured in terms of tensile flow stress at room temperature after recovery treatments between 80° and 200°C.

The major findings of the initial study included the following:

- Equivalent structural states in terms of identical stress-strain curves were obtained independent of recovery temperature, when specimens having the same cold-worked condition were recovered to equal values of fractional flow-stress recovery.
- For the higher three recovery temperatures, the Al-1.0% Mg alloy clearly experienced a greater degree of fractional flow-stress recovery than the high-purity base aluminum.
- For a given recovery treatment, the fractional flow-stress recovery was found to be independent of prestrain values between 0.04 and 0.14 for both the 99.995% Al and the Al-1% Mg alloy.
- Whereas concurrent elastic strain was concluded to have no effect on the rate of flow-stress recovery of the 99.995% aluminum, concurrent creep straining had a very significant effect. However, the activation energy of the recovery process was not found to be significantly different as a result of concurrent creep straining.

This part of the report presents the results of an extension of the initial study of the effect of solid-solution additions on the recovery behavior of aluminum. The effect of single, 0.1 atomic % additions of magnesium, copper, zinc, and silver on the recovery behavior of high-purity aluminum was studied at 80°, 120°, 160°, and 200°C under no-load conditions, and at 160°C under conditions of a creep stress.

## Section 2 EXPERIMENTAL PROCEDURE

### 2.1 TEST MATERIALS

The materials used in this study were a high-purity aluminum and four binary solid-solution aluminum alloys prepared from the high-purity base aluminum by the Alcoa Research Laboratory, New Kensington, Pennsylvania. The chemical analyses for these five test materials are summarized in Table 1. The solid solubility of the four solute additions in aluminum, along with the effect of each solute on the lattice parameter of aluminum, is presented in Table 2. All materials were received in the form of 0.125-in.-thick sheet material, as cold-rolled. Tensile specimens were cut in the rolling direction from the as-received sheets, using a tensilkut, high-speed pin router and template to produce the specimen geometry shown in Fig. 1. The recrystallization treatments and resulting grain size for each of the test materials are given in Table 3. All specimens were recrystallized after machining and prior to testing.

Table 1

CHEMICAL ANALYSES OF TEST MATERIALS  
(wt %)

Material	Alcoa Lot No.	Cu	Fe	Si	Mg	Zn	Ag	Solute Content (Atomic %)
99.99+% Al	196999-B	0.004	0.001	0.001	—	—	—	—
Al-Mg	252958-B	.005	.001	.001	0.09	0.001	—	0.100
Al-Cu	252959-B	.25	.001	.001	—	.001	—	0.104
Al-Zn	252961-B	.004	.001	.001	—	.23	—	0.094
Al-Ag	252960-B	.004	.002	.001	—	.001	0.39	0.097

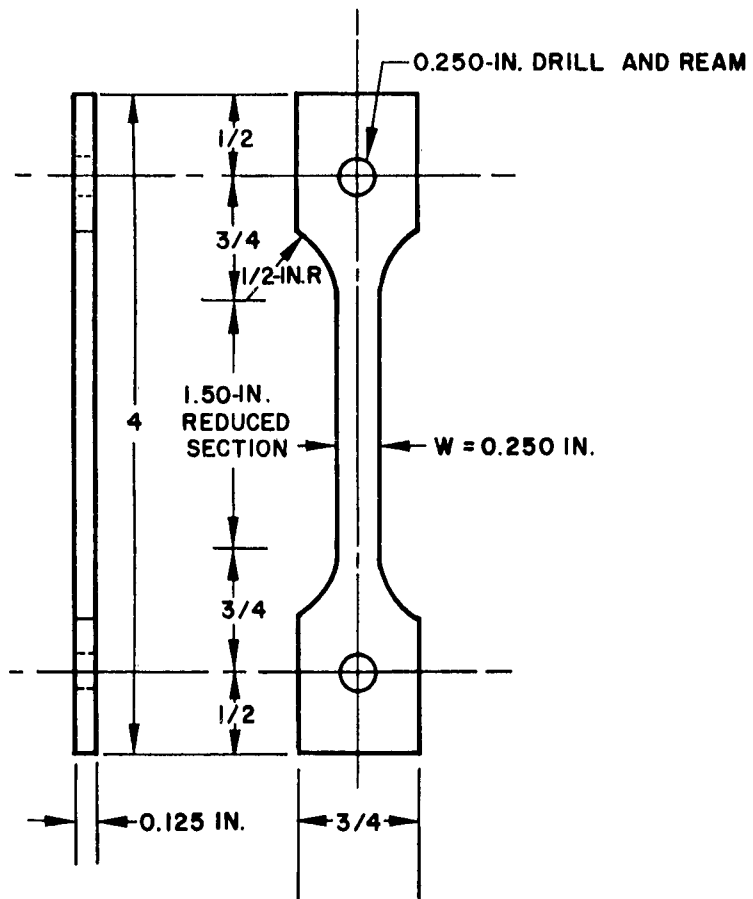


Fig. 1 Tensile Test Specimen Design

Table 2

ROOM-TEMPERATURE SOLID SOLUBILITY DATA AND CHANGE  
IN LATTICE PARAMETER OF ALUMINUM PER ATOMIC  
PERCENT SOLUTE

Solute	Solubility at Room Temperature (atomic %)	Change in Lattice Parameter per Atomic Percent of Solute (Kx unity)
Mg	3.22	+ 0.00350
Cu	0.23	- 0.00490
Zn	1.62	- 0.00068
Ag	0.19	0.00000

Table 3

RECRYSTALLIZATION TREATMENT

Material	Annealing Time (min) in Salt Bath at 450°C	Recrystallized Grain Size (mm)
99.99+Al	20	0.47
Al-Mg	25	.37
Al-Cu	25	.43
Al-Zn	20	.35
Al-Ag	20	.36

## 2.2 APPARATUS

The equipment used in this investigation consisted of three parts: (1) a means of performing and recording tensile stress-strain behavior at room temperature, (2) controlled temperature baths for recovery treatments of the prestrained specimens, and (3) equipment for application of selected stress levels during recovery and for measurement of creep strains.



The room-temperature straining of specimens, before and after recovery treatment, was accomplished with an Instron Testing machine which autographically recorded the load-deflection curve, using a 10,000-lb load cell. All tensile tests, both prior to and after recovery, were conducted at room temperature at a strain rate of about 0.03 per min. An assembly of the tensile specimen and extensometer, mounted in the Instron machine, is shown in Fig. 2. The extensometer consists of two linear-variable-differential transformers (LVDT's) mounted on the pull-bar, with one transformer core connected to the upper gage block and the other connected to the lower gage block. The net output of the two transformers was proportional to the extension between the two gage blocks. This output was amplified within the Instron and recorded autographically. The resulting least-counts in the autographically recorded load-deformation curve were equivalent to a strain of 0.002, and a stress of 60 psi in the case of the high-purity aluminum and of 150 psi in the case of the four alloys. The extensometer calibrations were checked during and upon completion of the program and were found to remain constant.

The constant-temperature baths used for the recovery treatments under no-load conditions are shown in Fig. 3. Four recovery baths were used at temperatures of 80°, 120°, 160°, and 200°C. Silicone oil was used for all four recovery baths. The bath temperatures were maintained constant to within  $\pm 1^\circ\text{C}$  by means of a mercury thermostat. For a few of the long time tests (approaching 1,000 hr), temperature variations slightly larger than this occurred.

For the purpose of investigating the effect of plastic strain upon recovery, two additional recovery baths were mounted on constant-load creep frames, as shown in Fig. 4. These baths were mounted on drill press columns so they could be raised to immerse the test specimen in the silicone oil. Specimens were loaded through 20-to-1 lever arms prior to application of the oil bath and were unloaded after oil quenching to near room temperature. The strain measurements for the recovery tests during concurrent creep straining were made using an optical cathetometer to determine small creep strains of the order of 0.0001.

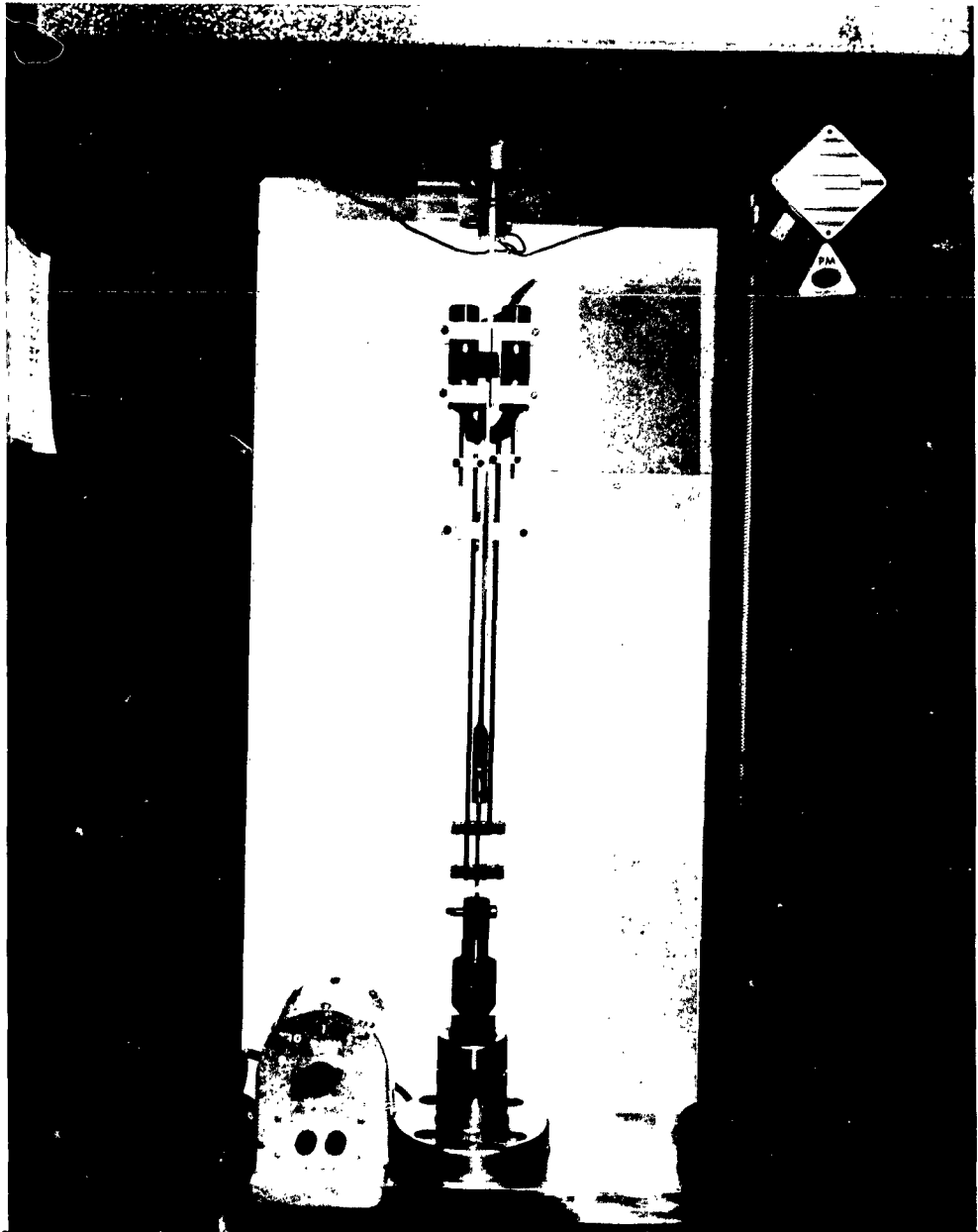


Figure 2. Tensile Specimen and Extensometer Assembly  
in Test Position

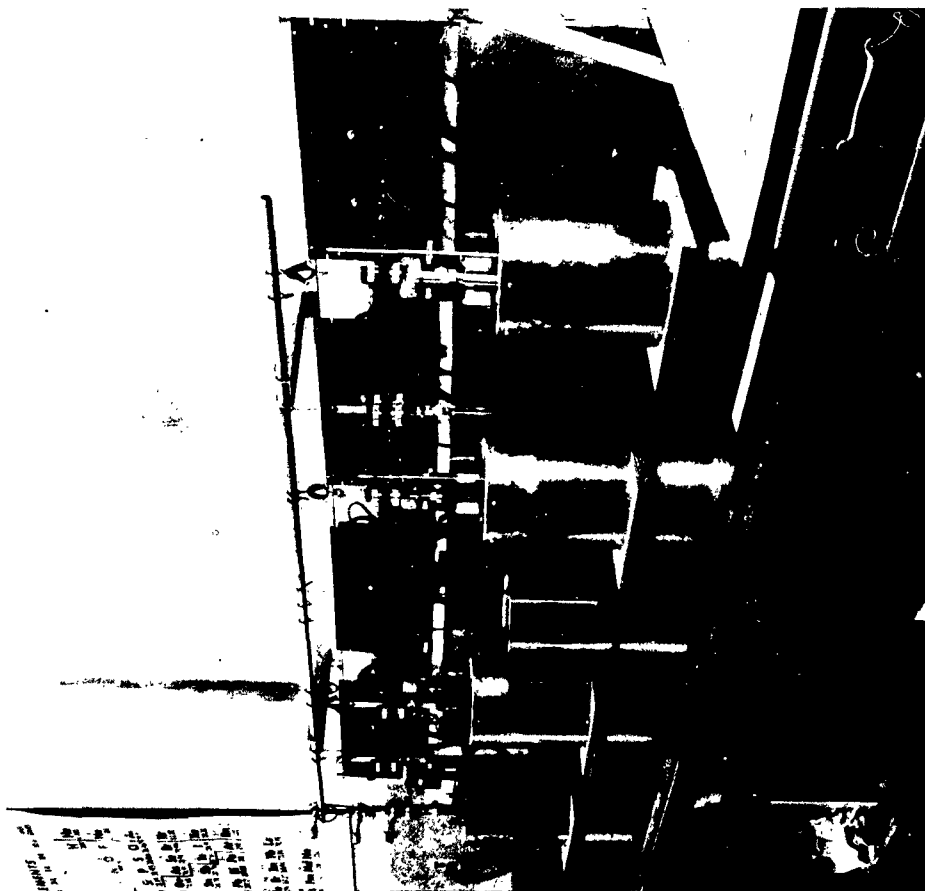


FIGURE 3. Constant Temperature Baths Used for Recovery Under No-Load Conditions

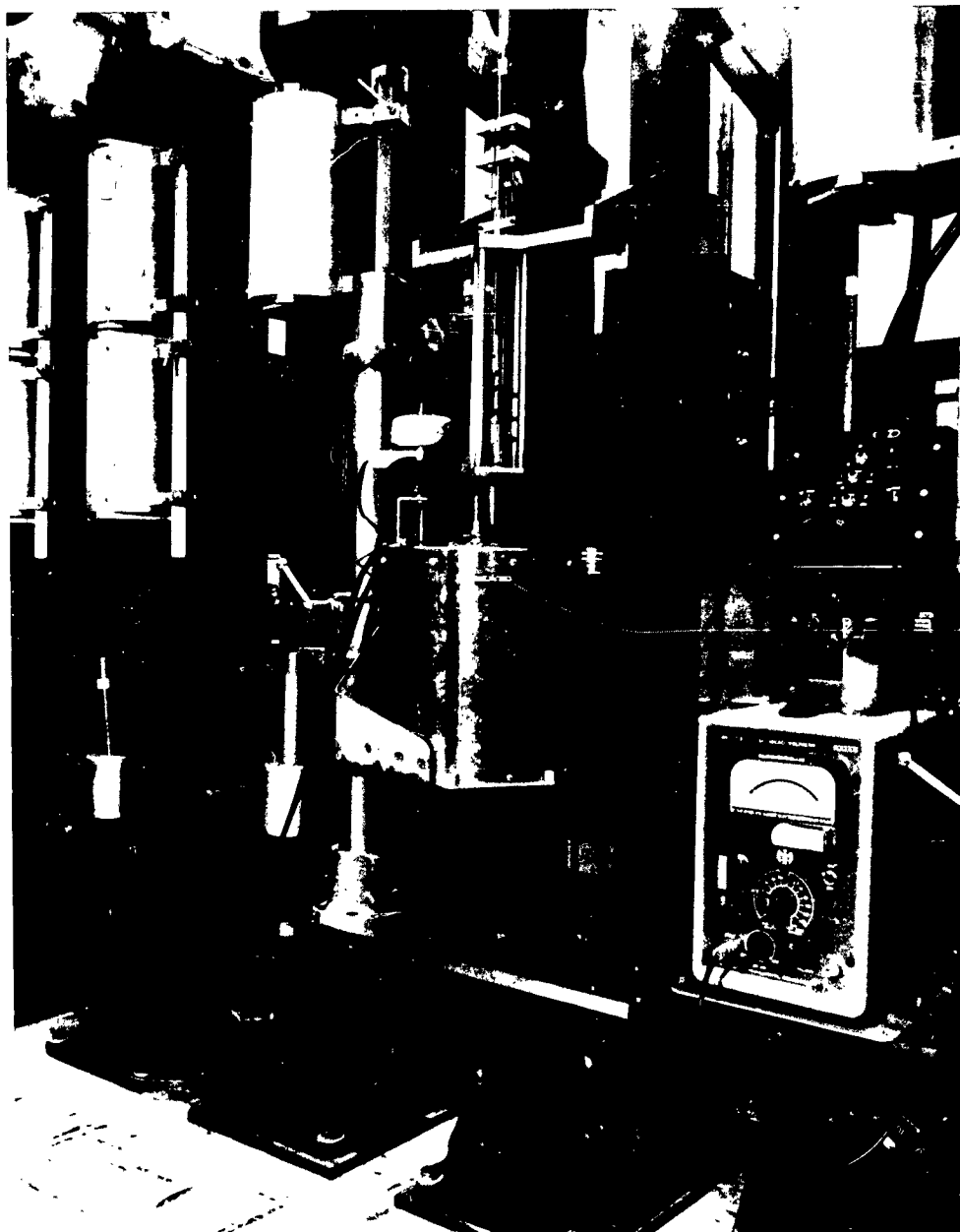


Figure 4. Experimental Setup for Studying Recovery Behavior  
Under Conditions of Concurrent Stress

At the outset of this program, a specimen was mounted in an extensometer and a thermocouple was spot-welded to the center of the gage section. Heating curves were obtained for each bath temperature so that the time-temperature path for the specimen to reach bath temperature was determined. After the results of longer tests had indicated the magnitude of the activation energy for recovery in the 80° to 200°C temperature range, it was possible to calculate a correction in recovery time necessary to subtract to obtain the total effective time at bath temperature. This time correction ranged from 1.0 to 1.8 min and was significant for only the shorter recovery treatments of 1 hr or less. The quenching operation was found to be rapid enough so that no correction was necessary for this operation.

### 2.3 METHOD OF EVALUATING RECOVERY

The degree of recovery after prestraining at room temperature was evaluated in terms of tensile properties by measuring the decrease in initial flow stress after various recovery treatments. Figure 5 shows schematically the effect of a recovery treatment on the true stress-true strain,  $\sigma - \epsilon$ , curve. The degree of recovery was evaluated in terms of fractional recovery  $f_r$ , where  $f_r$  is defined as the decrease in the flow stress due to the recovery treatment divided by the decrease experienced if the material recovered completely to the unstrained state. Thus, as illustrated in Fig. 5,

$$f_r = \frac{(\sigma_1 - \sigma_2)}{(\sigma_1 - \sigma_y)}$$

For the high-purity aluminum used in the first year's program (aluminum A), the initial yield stress  $\sigma_y$  upon straining the recrystallized material was very low — in some cases approaching zero. The values varied, presumably because of slight differences in handling the very soft material during the mounting of the extensometer. In calculating  $f_r$  for the recovery tests on aluminum A,  $\sigma_y$  was thus taken as zero. However, for the current study the high-purity aluminum which served as the base metal for the four binary alloys, the yield stress was significant and fairly constant at around

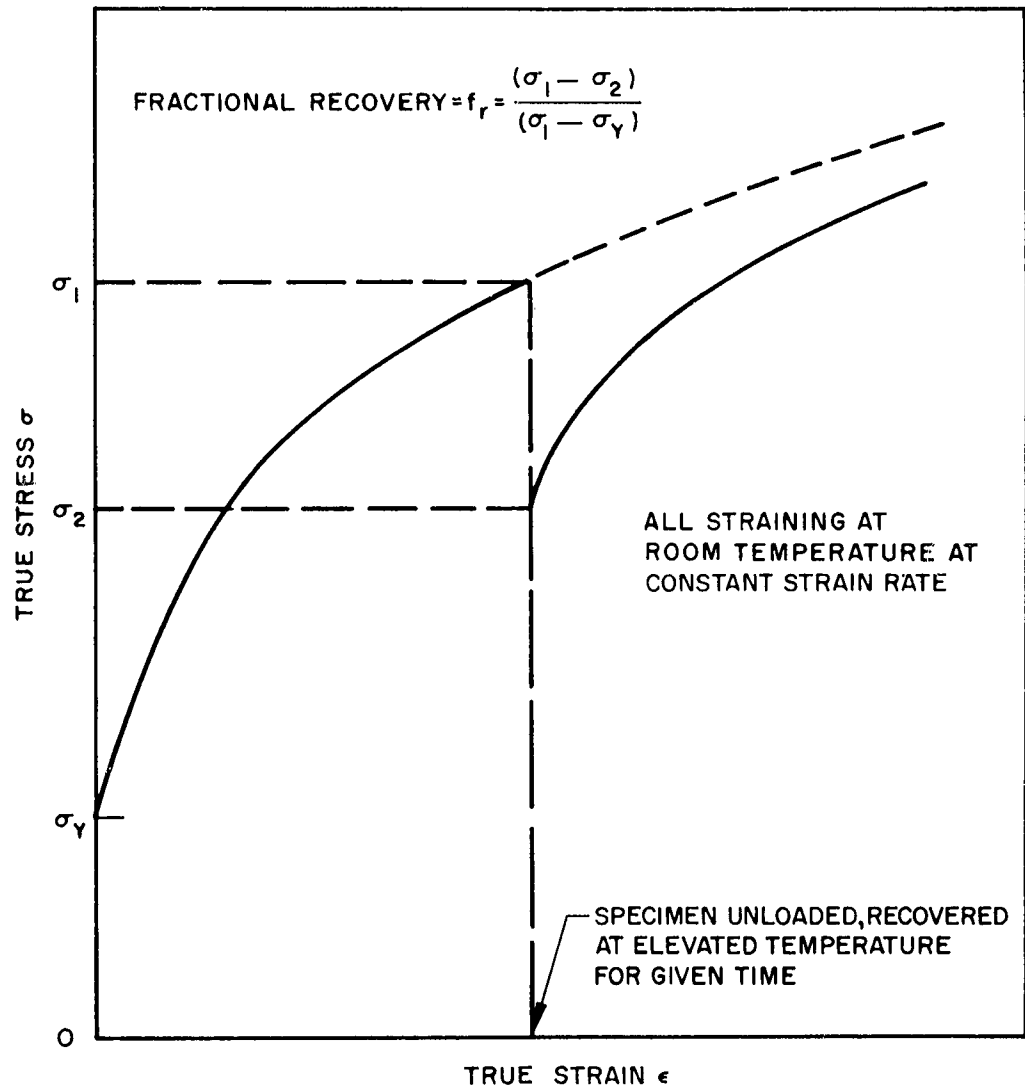


Fig. 5 Schematic Diagram Showing the Effect of Recovery on the Stress-Strain Curve and the Method Used To Evaluate the Degree of Recovery

600 psi. Thus, in the current study, the actual value of the initial yield strength was used in calculating  $f_r$  for the high-purity base and for the four alloys.

Several aluminum specimens were prestrained, unloaded for a short time at room temperature, and restrained. A slight drop – about equal to the width of the recorded ink line – was observed in the initial yield strength. This drop, attributed to a small amount of recovery at room temperature, was equal to an  $f_r$  value of about 0.003. Since at the lowest recovery temperature of 80°C and for the short recovery times the four alloys recovered about the same amount or less than the aluminum base material, the degree of recovery of the alloys at room temperature for short periods of time would not be expected to exceed an  $f_r$  value of 0.003.

Laue back-reflection studies which were conducted on the high-purity aluminum after 15% prestrain showed that no recrystallization was obtained after 1 hr at 450°C, giving assurance that only recovery occurred at the highest temperature of 200°C used in this investigation. Although no recrystallization occurred after 1 hr at 450°C for a specimen prestrained 15%, the as-received material which was in a severely cold-worked condition as indicated earlier was completely recrystallized at the same temperature in 20 min.

### Section 3

## EXPERIMENTAL RESULTS

All recovery tests were conducted on specimens which were prestrained at room temperature to 10% true strain. The tensile flow-stress data, before and after recovery treatment, were obtained from autographically recorded load-deformation curves. The technique of evaluating the degree of recovery in terms of the decrease in the initial flow stress due to recovery proved very satisfactory for all the aluminum alloys and resulted, in most cases, in a well-defined initial flow stress. In the most poorly defined cases, the uncertainty in the initial flow stress was still less than  $\pm 5\%$ .

### 3.1 RECOVERY BEHAVIOR OF THE HIGH-PURITY BASE ALUMINUM

The recovery behavior of the high-purity aluminum which served as the base for the four binary alloys is summarized in Fig. 6 in terms of fractional flow-stress recovery,  $f_r$ , versus the log of the recovery time for the four recovery temperatures. This aluminum is referred to as aluminum B.

For the lower two recovery temperatures, the data resulted in linear, almost parallel, lines. This was also true for the 160°C data up to about 100 hr recovery time, after which a break in the  $f_r$  versus  $\log t$  curve occurred, where the recovery process appeared to stop. At 200°C, the recovery of flow stress was initially very rapid, reaching a constant value during the first 12 min. No additional recovery appeared to take place after 1/2 hr for times up to 1,000 hr.

The recovery behavior of the high-purity aluminum B, particularly at the highest recovery temperature of 200°C, was quite different from that observed for the aluminum A, which had the same nominal purity. Whether the observed differences were due to the reported differences in impurities is not known; however, the aluminum A was reported to contain less copper (0.001 versus 0.004) and more iron (0.002 versus 0.001) than aluminum B.



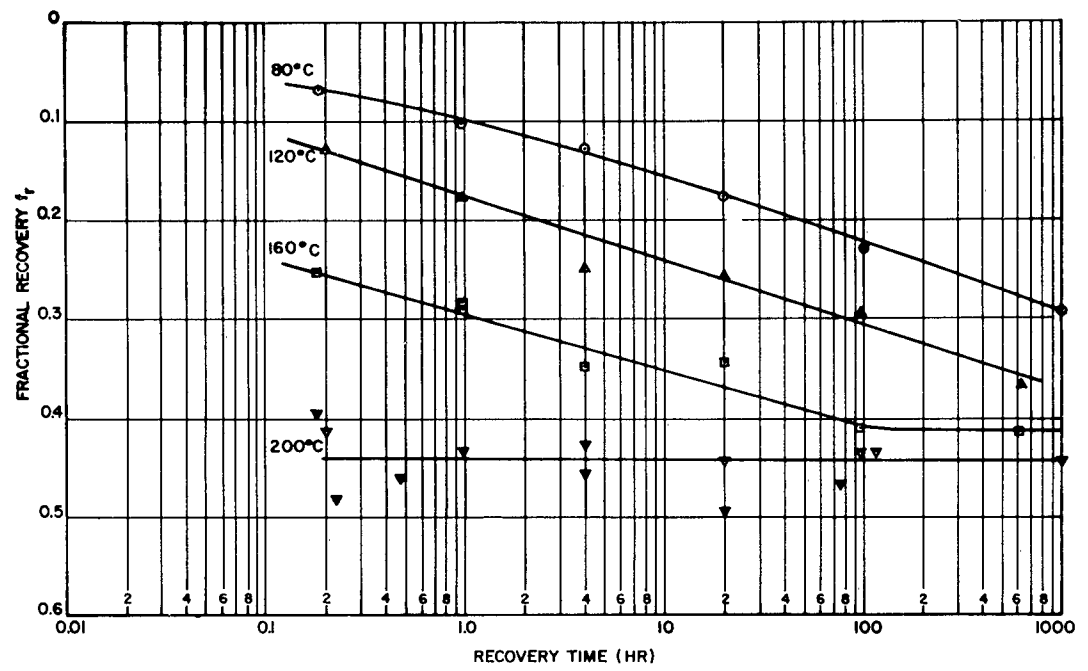


Fig. 6 Fractional Recovery as a Function of Recovery Time for 99.99% Aluminum at Four Recovery Temperatures

### 3.2 RECOVERY BEHAVIOR OF THE ALUMINUM ALLOYS

The recovery data for the four binary alloys are summarized in Figs. 7 through 10 for the four recovery temperatures and for recovery times of about 0.2 to 1,000 hr. All recovery data presented in these figures were obtained under no-load conditions.

The data of Fig. 7, for the Al-0.1 atomic % Mg alloy, indicate that the fractional recovery of flow stress proceeded in a linear manner with log recovery time with the exception of the highest recovery temperature where recovery of the flow stress appeared to stop after about 100 hr at an  $f_r$  value of about 0.48. The curve representing the 80°C recovery data has a considerably lower slope than the curves for the higher three recovery temperatures.

Figure 8 summarizes the recovery data for the Al-0.1 atomic % Cu alloy. The general trends are the same as for the Al-0.1% Mg alloy except that the Al-0.1% Cu alloy exhibited a greater degree of recovery at the three higher recovery temperatures, and also exhibited plateaus in the  $f_r$  versus log  $t$  curves at both 160° and 200°C. The  $f_r$  value at which recovery appeared to cease was 0.54 and 0.58 for recovery temperatures of 160° and 200°C, respectively.

The  $f_r$  versus log  $t$  curves for the Al-Zn alloy, summarized in Fig. 9, are all about parallel over their linear range, in contrast to the lower slopes exhibited by the Al-Mg and Al-Cu alloys at the 80° recovery temperature. At the longer recovery times, all three curves for the higher temperatures show a plateau where recovery appeared to stop. This occurred at  $f_r$  values of about 0.37, 0.46, and 0.53 for recovery at 120°, 160°, and 200°C, respectively. These plateaus indicate that a constant recovery structure is reached during the recovery process at a given temperature. A higher recovery temperature results in a different constant recovery structure which is weaker and thus gives rise to a larger value of  $f_r$ . Each of these constant recovery structures appears to be metastable and characteristic of the specific recovery conditions, as will be evident later.

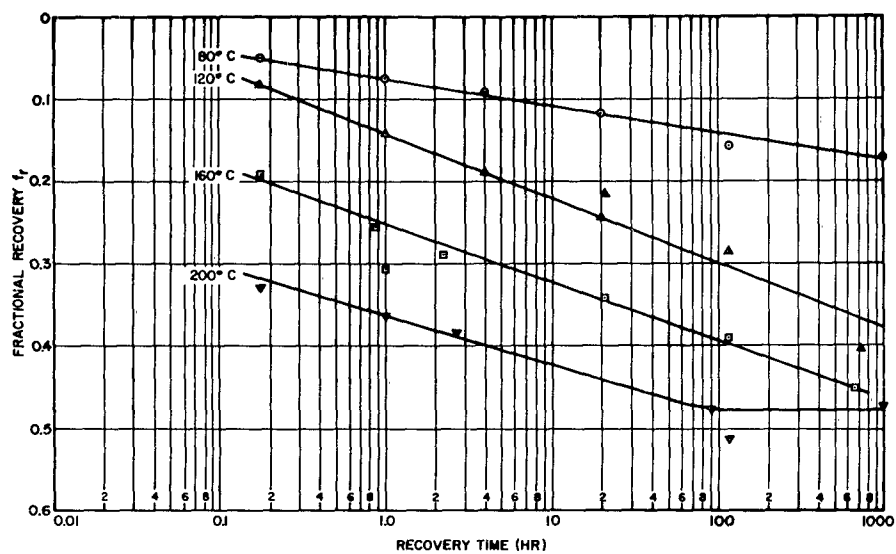


Fig. 7 Fractional Recovery as a Function of Recovery Time for Al-0.1% Mg Alloy at Four Recovery Temperatures

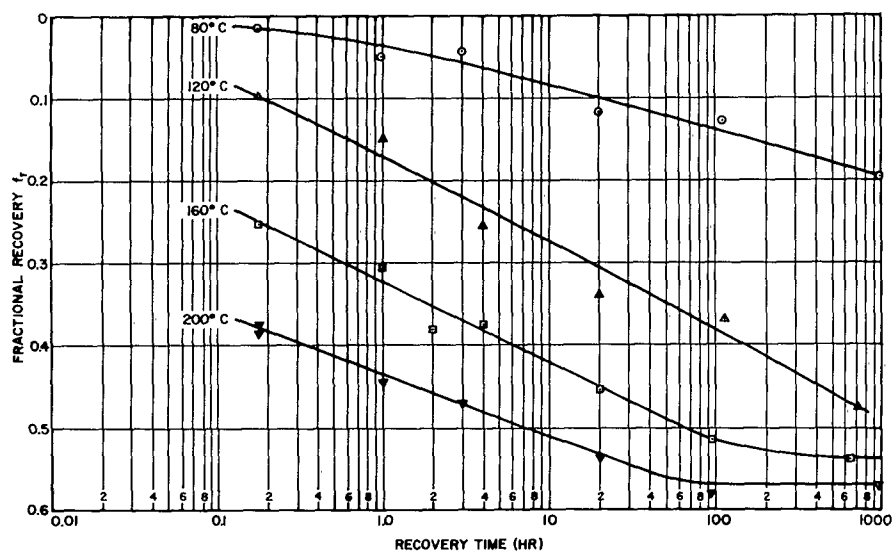


Fig. 8 Fractional Recovery as a Function of Recovery Time for Al-0.1% Cu Alloy at Four Recovery Temperatures

The recovery data for the Al-Ag alloy are summarized in Fig. 10. It is immediately apparent that at the higher recovery temperatures some strengthening process was occurring, as a point was reached where the  $f_r$  values showed an increase with increasing recovery time. Also at the lower recovery temperatures for times less than 1 hr, the curves are concave upward; this is the reverse trend exhibited by the curves for all the other test materials, which were concave downward at 80°C and either linear or concave downward at 120°C. The latter observation could indicate that even for the 80°C recovery temperature and very short recovery times, the strengthening process was already occurring. An additional point of interest is the fact that for the higher two recovery temperatures the maximum  $f_r$  achieved by the Al-Ag alloy was greater than that for any of the other test materials. The very processes which led to the strengthening effect could have accelerated the reduction of the stored internal energy due to cold-work and thus increased the actual degree of recovery. Thus, it is possible that even smaller values of  $f_r$  would have resulted had no strengthening process been taking place. Because of the possible interactions of the strengthening and recovery processes, in the case of the Al-Ag alloy, any comparison of the effect of the silver addition as a simple solid-solution addition on the recovery behavior of the base aluminum would be questionable. With this in mind, the curves representing the Al-Ag alloy will be included in certain figures only for general interest.

The recovery data for the high-purity base aluminum and the four binary alloys are presented in Figs. 11 through 14 to allow comparison of the five test materials in terms of  $f_r$  versus  $\log t$  at constant recovery temperatures. The Al-Ag alloy curves are included in these figures for completeness.

At the lowest recovery temperature studied, 80°C, the curves summarized in Fig. 11 indicate that the Al-Cu and Al-Mg alloys exhibited less recovery than the unalloyed aluminum over the entire range of recovery times.

The Al-Ag alloy initially exhibited the same degree of recovery at 80°C as the aluminum. However, after 1 hr, the Al-Ag alloy started to deviate from the unalloyed aluminum curve and showed less recovery, finally joining the curves for the Al-Mg

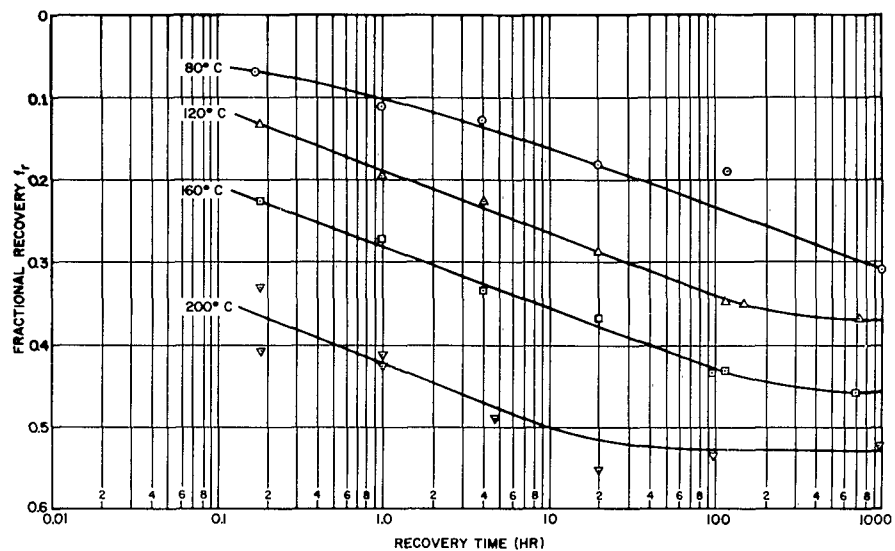


Fig. 9 Fractional Recovery as a Function of Recovery Time for Al-0.1% Zn Alloy at Four Recovery Temperatures

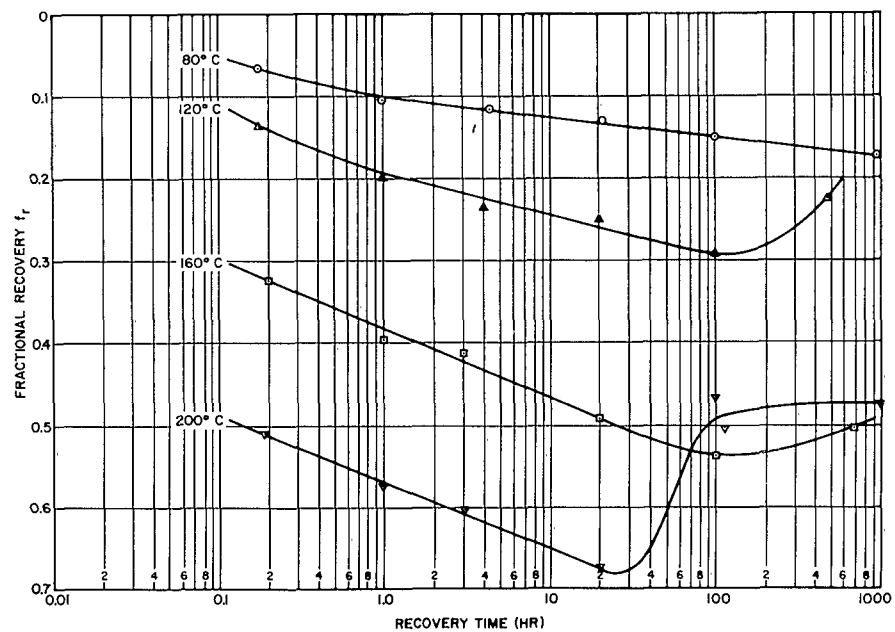


Fig. 10 Fractional Recovery as a Function of Recovery Time for Al-0.1% Ag Alloy at Four Binary Temperatures

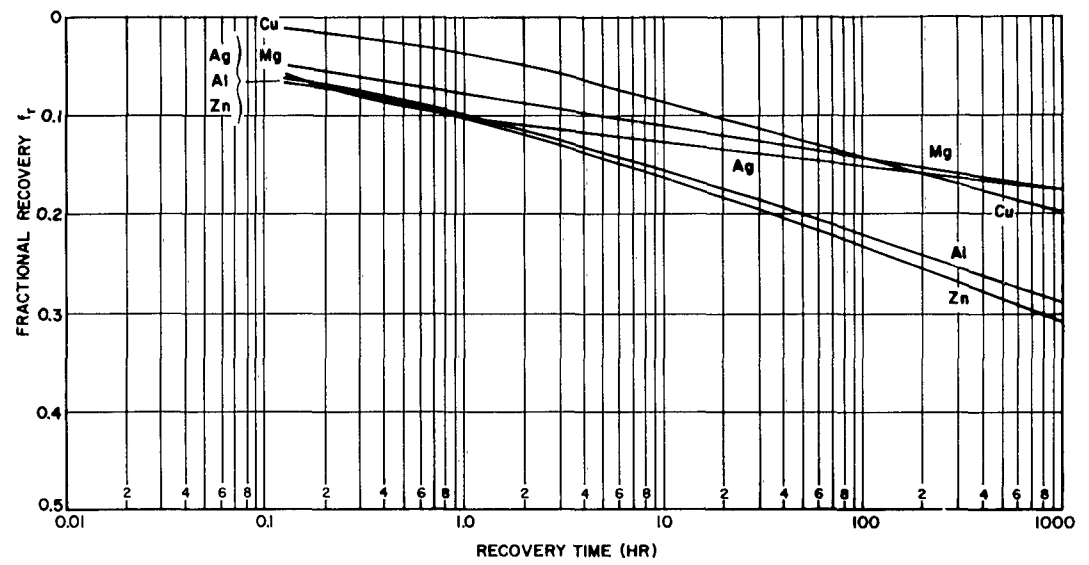


Fig. 11 Fractional Recovery Versus Recovery Time for Aluminum and the Four Binary Aluminum Alloys at 80°C

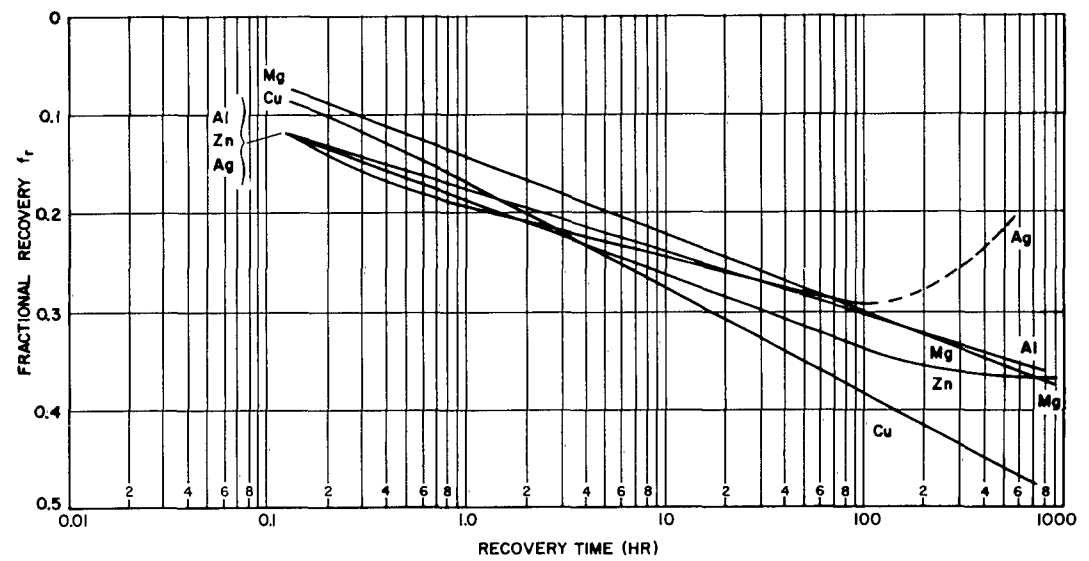


Fig. 12 Fractional Recovery Versus Recovery Time for Aluminum and the Four Binary Aluminum Alloys at 120°C

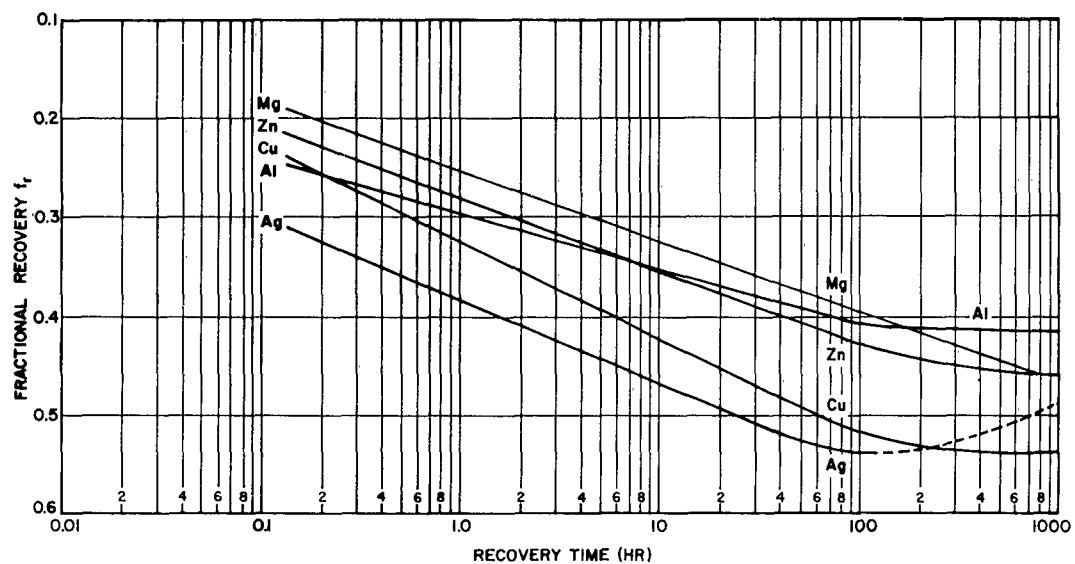


Fig. 13 Fractional Recovery Versus Recovery Time for Aluminum and the Four Binary Aluminum Alloys at 160°C

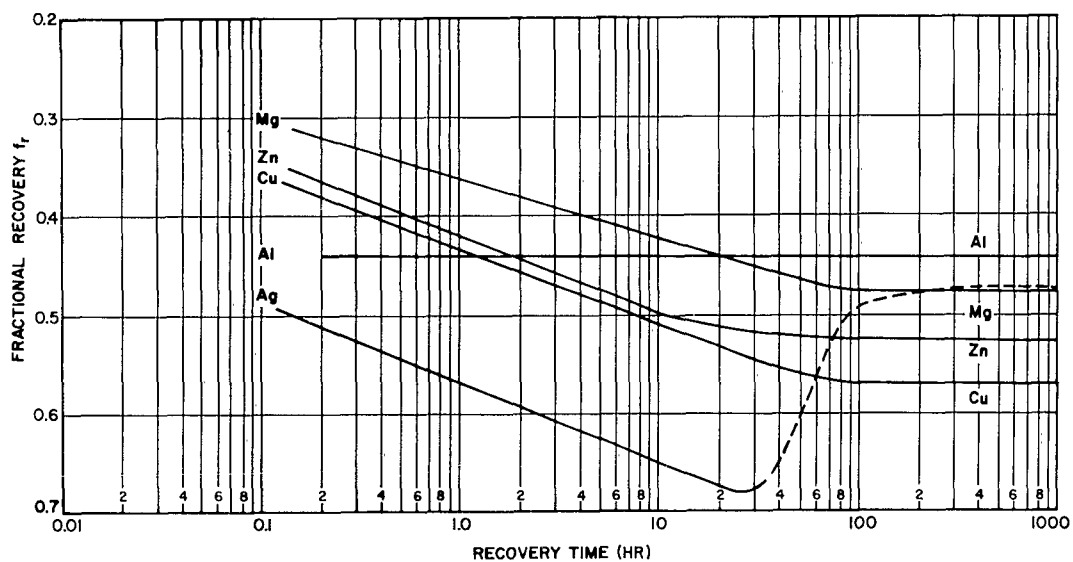


Fig. 14 Fractional Recovery Versus Recovery Time for Aluminum and the Four Binary Aluminum Alloys at 200°C

and Al-Cu alloys. The authors believe this behavior in the case of the Al-Ag alloy is due to the aforementioned occurrence of a strengthening process during recovery. The behavior of the Al-Zn alloy follows very closely that of the unalloyed aluminum at 80°C.

At 120°C, as shown in Fig. 12, the Al-Mg and Al-Cu alloys initially exhibited less recovery than the unalloyed aluminum. Although all three materials had almost linear  $f_r$  versus  $\log t$  curves, owing to differences in their slopes the curve for the Al-Mg alloy crossed under the aluminum curve after about 150 hr, and the curve for the Al-Cu alloy crossed under the aluminum curve after only 1-1/2 hr. After about 4 hr of recovery at 120°C, the Al-Cu alloy exhibited a greater degree of recovery than any of the other test materials.

Figure 13 presents the data for the five test materials for recovery at 160°C. The Al-Mg alloy, the Al-Zn alloy, and interestingly the Al-Ag alloy all resulted in about parallel  $f_r$  versus  $\log$  time curves up to about 100 hr of recovery time. The curve for the unalloyed aluminum was flatter, cutting across the Al-Cu, Al-Zn, and Al-Mg alloys and at times exceeding 160 hr, showed less recovery than the four alloys. For times longer than 0.2 hr, the Al-Cu alloy exhibited a greater degree of recovery than the other materials, excluding the Al-Ag alloy.

The data for the highest recovery temperature, 200°C, are presented in Fig. 14. The  $f_r$   $\log$  time curves for all four alloys are linear and nearly parallel up to the time when the recovery process appeared to stop, and the curves reach plateaus. This occurred at about 100 hr for the Al-Mg alloy and the Al-Cu alloy, and about 50 hr for the Al-Zn alloy. The curve for the Al-Ag alloy goes through a minimum at about 30 hr. The  $f_r$  versus  $\log$  time curve for the unalloyed aluminum at 200°C is indeed anomalous when compared with the curves for the four alloys. The base aluminum recovered to a fractional flow stress value of about 0.44 during the first 12 min of recovery treatment, with no additional recovery for the next 1,000 hr. The curve for the high-purity aluminum thus proceeds to cross the curves for the Al-Cu, Al-Zn, and Al-Mg alloys and after recovery times greater than 20 hr exhibits less recovery than the alloys. (The Al-Ag alloy is excepted for reasons previously discussed.) For recovery times



longer than 20 hr at 200°C, the relative order for increasing degree of recovery is (1) unalloyed aluminum, (2) Al-Mg alloy, (3) Al-Zn alloy, and (4) Al-Cu alloy.

In summary, the data presented in Figs. 11 through 14 indicate that at the higher recovery temperatures of 120°, 160°, and 200°C, and for the longer recovery times, the three alloys under consideration, Al-Mg, Al-Zn, and Al-Cu, all experienced a greater degree of recovery than the high-purity base aluminum. Of these three alloys, the Al-Cu alloy clearly exhibited the greatest degree of recovery.

These observations are somewhat unexpected, as they are in conflict with the frequently stated concept that those solid solution additions which are most effective in inhibiting recovery are the most effective in increasing the elevated temperature strength. Intuitively, this statement would be accepted as reasonable. Solid-solution additions which are most effective in inhibiting the softening process would be expected to be the most effective for imparting elevated temperature strength. However, previous investigations of binary solid-solution additions to aluminum<sup>(3,4)</sup> have shown copper to be the most effective strengthening addition. The relative order of decreasing effectiveness, on the basis of equal atomic percent additions to aluminum, has been reported to be copper, magnesium, silver, and zinc, for both tensile properties<sup>(3)</sup> and creep properties.<sup>(4)</sup>

The relative order of solid-solution strengthening was determined for the four binary alloys used in this study in terms of tensile stress-strain curves at 160°C. These curves are presented in Fig. 15, where each curve represents an average curve for two tensile tests. The 0.1% copper addition is clearly the most effective strengthener, with 0.1% magnesium next, followed by 0.1% zinc, and finally the 0.1% silver addition which resulted in about the same stress-strain curve as for aluminum. Preliminary creep tests on the four binary alloys at 160°C and 3,000 psi placed the binary alloys in order of decreasing creep resistance as Al-Cu, Al-Mg, Al-Ag, and Al-Zn, which is in agreement with the earlier referenced creep study<sup>(4)</sup> which was conducted at 150°C.

In attempting to understand the role of the solute atom in the recovery process and in the solid-solution strengthening process, it should be pointed out that a direct

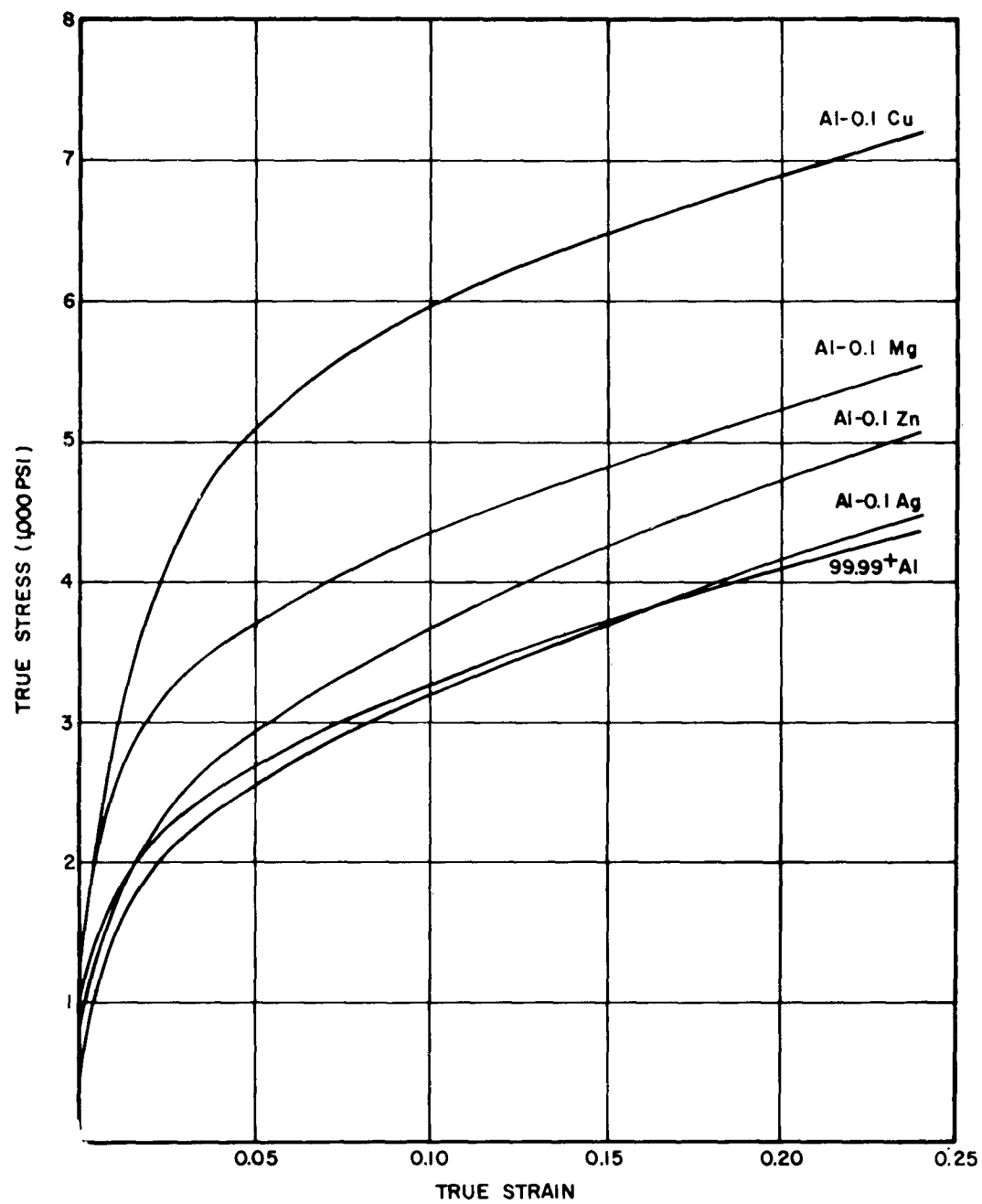


Fig. 15 True Stress - True Strain Curves for Aluminum and the Four Binary Aluminum Alloys at 160°C

correlation between recovery and elevated temperature strength is not demanded, even though it would seem reasonable for such a relationship to exist. Indeed the data presented clearly indicate that the Al-Cu alloy, which was the strongest alloy in both tension and creep at 160°C, also experienced the greatest degree of recovery at the same temperature. This does not say that the Al-Cu alloy would not have been stronger had it experienced less recovery. The statement that might apply is that the Al-Cu alloy exhibited the greatest elevated temperature strength of the materials studied in spite of the fact that it experienced the greatest degree of recovery.

One thing which should be noted at this time is that even though the Al-Cu alloy exhibited a greater fractional flow-stress recovery, it still possessed a higher value of initial flow stress after a given recovery treatment than the unalloyed aluminum or the other alloys under discussion: Al-Mg and Al-Zn alloys. To show this more clearly, two figures showing recovery data at 160°C are presented. Figure 16 shows the actual drop in flow stress during recovery ( $\sigma_1 - \sigma_2$ ) for aluminum and the three alloys, Al-Mg, Al-Cu, and Al-Zn, recovered at 160°C. As would be expected, these curves show the same general trends previously shown by the  $f_r$  versus log time curves for the same materials. Somewhat greater scatter is apparent in the data points for any one curve in the ( $\sigma_1 - \sigma_2$ ) versus log time plot, since one of the advantages of using the  $f_r$  or  $(\sigma_1 - \sigma_2)/(\sigma_1 - \sigma_y)$  parameter is the reduction of scatter due to sampling differences. The curves of Fig. 16 clearly show that the Al-Cu alloy experienced the greatest decrease in flow stress during recovery over the entire range of recovery times studied. For example, during 100 hr of recovery at 160°C the Al-Cu alloy experienced a decrease in flow stress of 3,700 psi or 52% of the increase in flow stress due to the prior 10% prestrain. The high-purity aluminum, for the same recovery treatment, experienced a decrease in flow stress of 2,000 psi, or only 41% of the increase in flow stress due to the prior 10% prestrain.

Figure 17 shows the actual flow stress after recovery ( $\sigma_2$ ) at 160°C for the same four test materials. Even though the Al-Cu alloy had experienced a greater absolute decrease and percentage decrease in flow stress during recovery, its recovered value was still above the other curves until after about 70 hr when they became about equal to the values

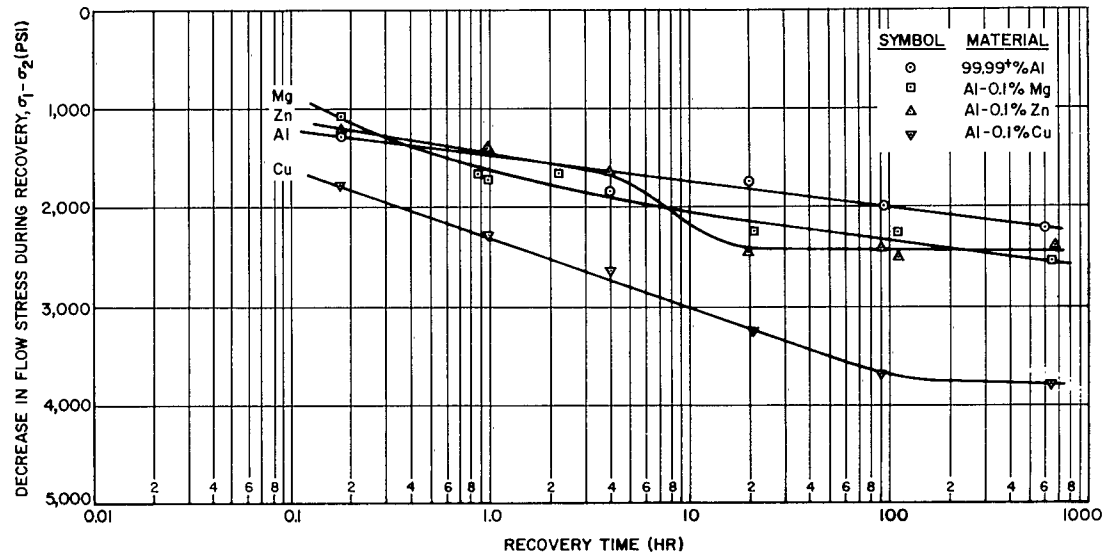


Fig. 16 Decrease in Room-Temperature Flow Stress During Recovery at 160° C for Aluminum and Three Binary Aluminum Alloys

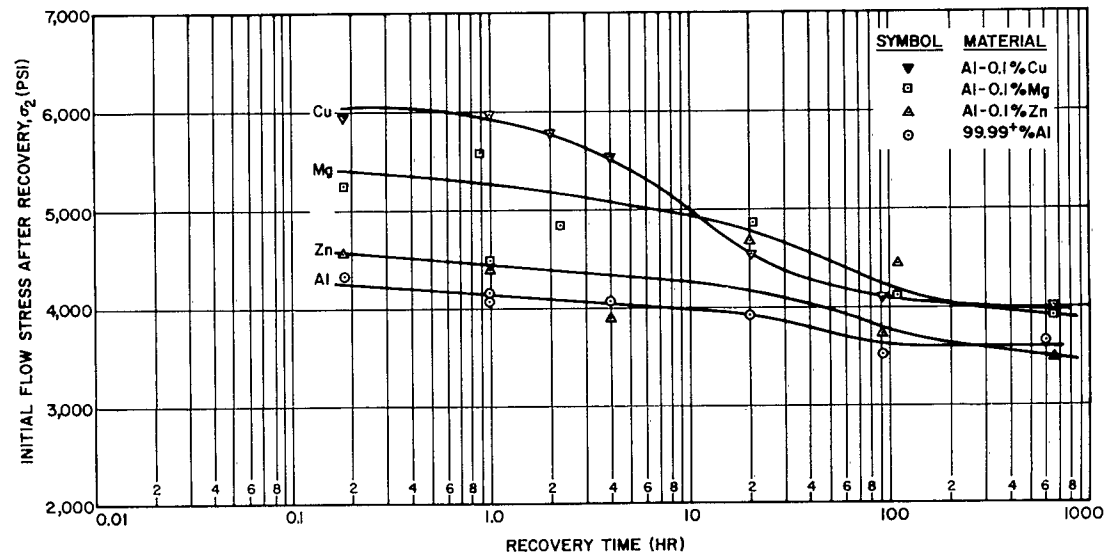


Fig. 17 Initial Flow Stress After Recovery as a Function of Recovery Time at 160° C for Aluminum and Three Binary Aluminum Alloys

for the Al-Mg alloy. For this plot of  $\sigma_2$  versus  $\log t$ , the full variation due to sampling differences is apparent.

### 3.3 RECOVERY BEHAVIOR OF THE HIGH-PURITY ALUMINUM AND THE FOUR BINARY ALLOYS UNDER CONDITIONS OF CONCURRENT PLASTIC STRAIN

An additional point for consideration is the effect which plastic strain would have on the recovery process of the different alloys. Results reported during the first year of this study showed that the recovery of high-purity aluminum was greatly accelerated during creep straining. It is possible that different alloy additions would behave differently under conditions involving strain. Since the tensile and creep tests at elevated temperatures were under an applied stress causing strain, it may be quite inaccurate to compare no-load recovery behavior of the various alloys with their relative strengthening effect in tension and creep.

To determine the relative recovery behavior during straining, a series of tests was conducted at 160°C on the base aluminum and the four binary alloys under a stress of 1,900 psi. In each case, the recrystallized specimen was prestrained 10% at room temperature; the specimen and extensometer assembly was then placed in a creep unit (Fig. 4) and loaded to a stress of 1,900 psi; and the recovery bath was raised into position. Following the recovery treatment under stress, the specimen assembly was returned to room temperature, transferred to the tensile machine, and finally strained at room temperature. The fractional flow-stress recovery was evaluated from the decrease in initial flow stress as previously described.

The results of these recovery tests are presented in Fig. 18 for the unalloyed aluminum and in Figs. 19 through 22 for the four binary alloys. In each figure, the upper solid curve represents the fractional recovery evaluated under no-load conditions at 160°C, and the lower solid curve and data points the recovery under a creep stress of 1,900 psi at the same temperature, 160°C. In all cases, the creep strain accelerated the recovery process and caused an appreciable increase in the total recovery. In all cases, the strains were less than 0.010 after 100 hr of creep-recovery. The lower dashed curve on these figures represents the fractional recovery evaluated at 200°C

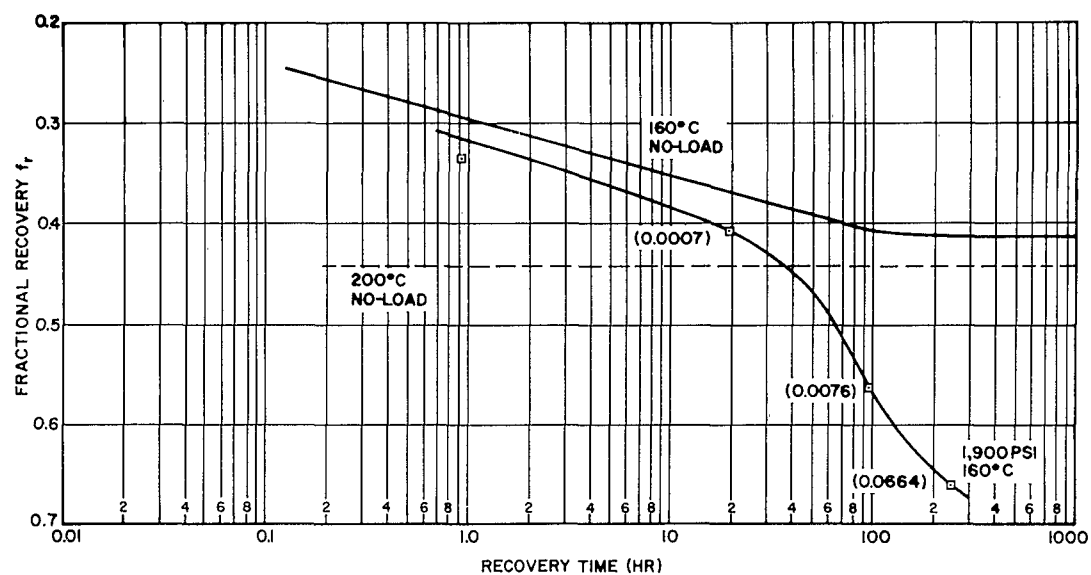


Fig. 18 Effect of Creep Strain at a Stress of 1,900 psi on the Recovery of 99.99% Aluminum at 160°C

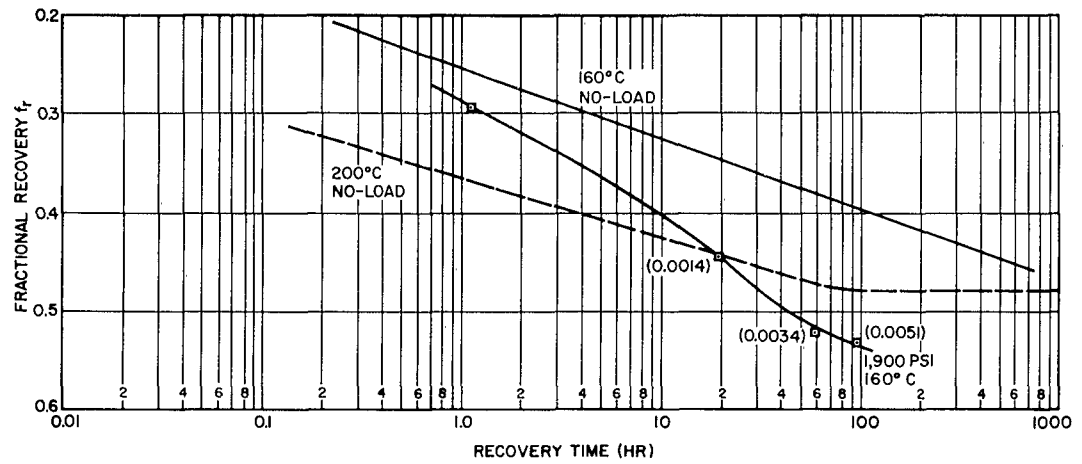


Fig. 19 Effect of Creep Strain at a Stress of 1,900 psi on the Recovery of the Al-0.1% Mg Alloy at 160°C

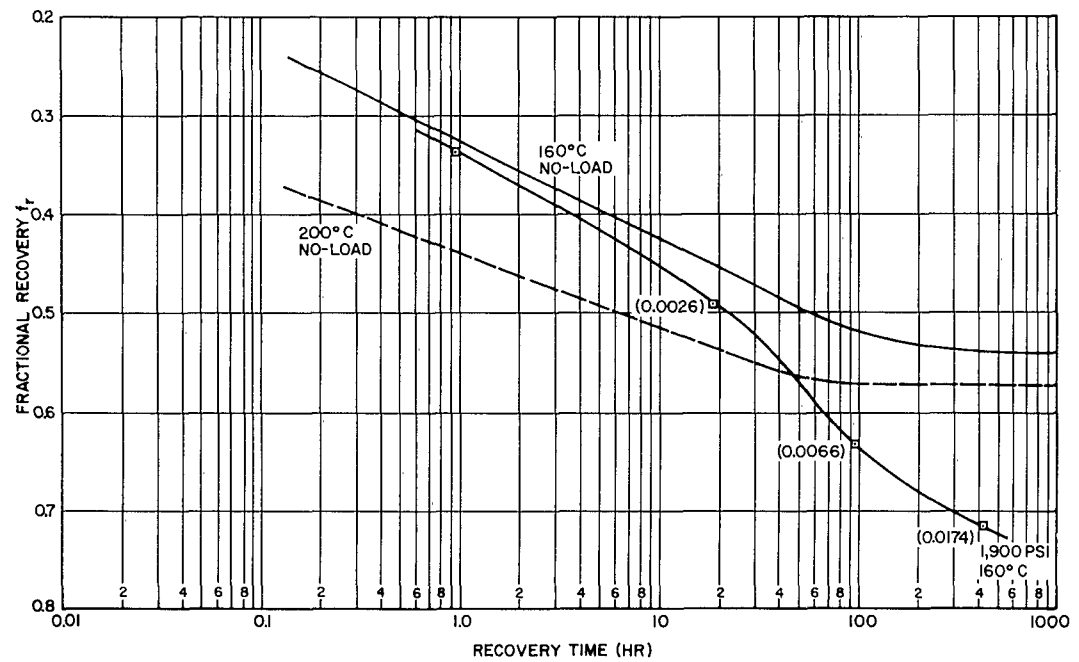


Fig. 20 Effect of Creep Strain at a Stress of 1,900 psi on the Recovery of the Al-0.1% Cu Alloy at 160°C

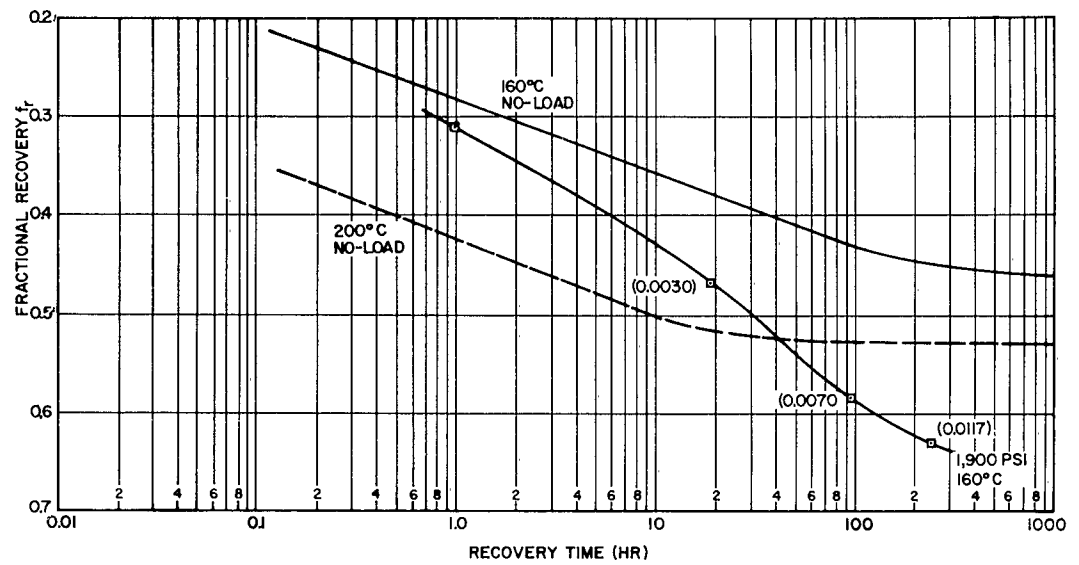


Fig. 21 Effect of Creep Strain at a Stress of 1,900 psi on the Recovery of the Al-0.1% Zn Alloy at 160°C

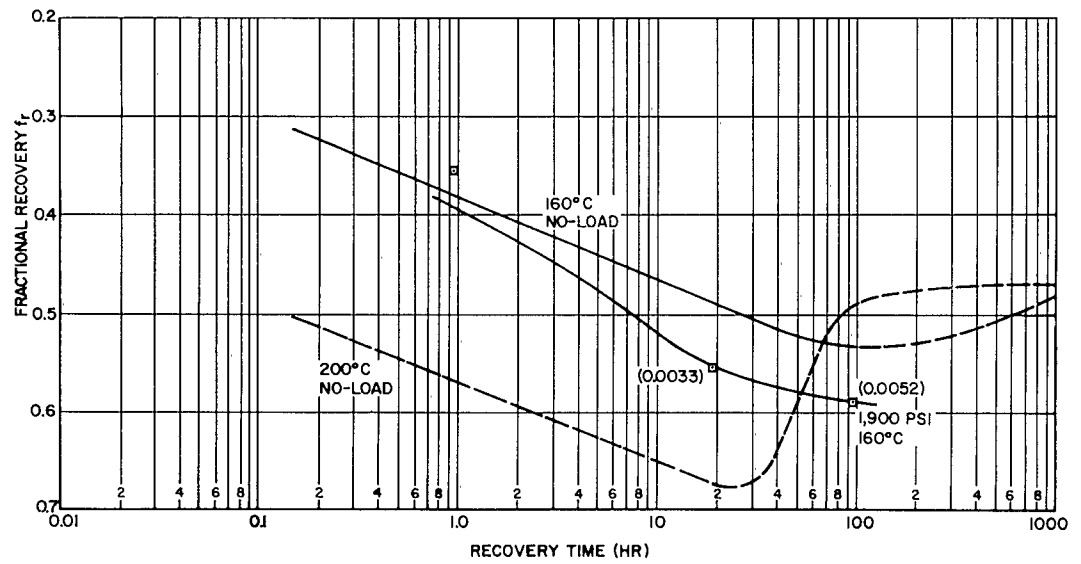


Fig. 22 Effect of Creep Strain at a Stress of 1,900 psi on the Recovery of the Al-0.1% Ag Alloy at 160°C



under no-load conditions. These 200°C recovery curves have been included to help emphasize the effectiveness of small strains in accelerating the recovery process. In all cases, strains of less than 0.005 during recovery at 160°C caused a greater increase in recovery than a 40°C increase in recovery temperature. The metastable recovery states reached during no-load recovery at 160° and 200°C were readily exceeded, in terms of  $f_r$  value, during recovery at 160°C concurrent with small creep strains.

The recovery data under concurrent creep strain at 160°C for all the alloys are summarized in Fig. 23, where the total fractional flow-stress recovery is plotted versus log recovery time. The curve for the unalloyed aluminum does not follow the general trend exhibited by the curves for the alloys; however, this may be due in part or in whole to one erroneous point, either 1 hr or 20 hr. Also, the Al-Ag alloy curve is included here only for completeness. A comparison of the curves for the three alloys of interest shows the following order of increase of total recovery: Al-Mg, Al-Zn, Al-Cu. Thus, these three alloys exhibited the same relative order of recovery under conditions of creep straining as they did under no-load conditions.

It is interesting to note that the order of increasing fractional recovery due to the different solute additions – Mg, Zn, and Cu – is also the order of decreasing solid solubility. Also, with reference to Table 3, magnesium causes a strong expansion, zinc a weak contraction, and copper a strong contraction of the aluminum lattice.

The increased amount of recovery during creep straining over that experienced during no-load recovery,  $\Delta f_c$ , as a function of the amount of creep strain is presented in Fig. 24 for the four binary alloys and the base aluminum. The data points given in Fig. 24 are based upon the curves presented in Figs. 18 through 22. The numbers given in parentheses beside the data points in Figs. 18 through 22 indicate the creep strain which occurred during 160°C under 1,900 psi for each of the tests. Values are not given for the shortest recovery tests of 1 hr because of some question that the specimen-extensometer assemblies were truly at thermal equilibrium for the readings taken at the beginning and end of test.

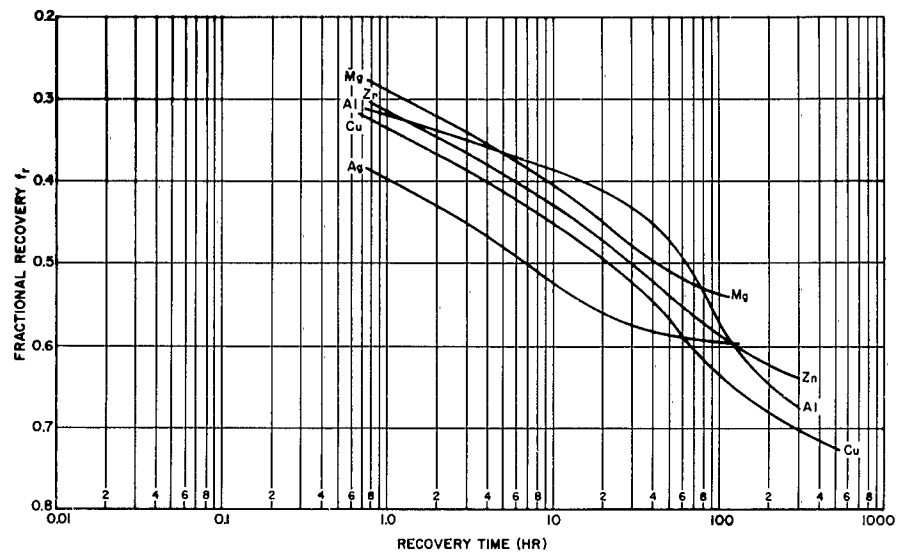


Fig. 23 Total Fractional Recovery During Creep Strain at a Stress of 1,900 psi for Aluminum and the Four Binary Alloys at 160°C

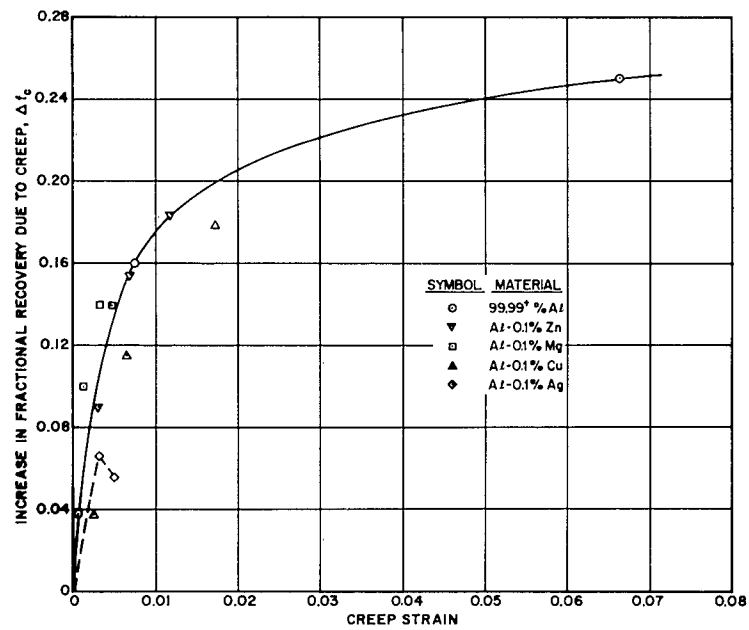


Fig. 24 Increase in Fractional Recovery Due to Creep as a Function of Creep Strain for Aluminum and the Four Binary Aluminum Alloys Under a Stress of 1,900 psi at 160°C

The data of Fig. 24 indicate that the additional increment of recovery due to creep strain increased very rapidly during the initial creep strain for all test materials. A strain of 0.005 resulted in an increase in the fractional recovery of about 0.14. The  $\Delta f_c$  versus creep-strain curve drops off rapidly; a tenfold increase in creep strain, 0.050, less than doubled the value of  $\Delta f_c$ . Whether a real difference exists between the different alloys in the  $\Delta f_c$  values for a given creep strain is not clear from the available data. The points for the Al-Mg alloy fall above the general curve, and those for the Al-Cu alloy below. The points for the Al-Ag alloy initially show an increase in the  $\Delta f_c$  value with strain, followed by a decrease with additional strain. This may indicate that the strengthening process in the Al-Ag alloy was being accelerated due to the concurrent strain; however, such a conclusion is not warranted on the basis of these preliminary data. In any case, the fractional recovery of aluminum and the Al-Mg, Al-Zn, and Al-Cu alloys is strongly accelerated by creep strain, and the different alloys appear to be about equally affected.

It is not possible to determine from this study the possible relationship between total creep strain and recovery time as they affect the increased fractional recovery  $\Delta f_c$ . In other words, is the mere presence of a very small concurrent strain the important factor over a given isothermal recovery period, or is the rate of strain also an important variable? Tests conducted at constant strain rates for fixed recovery treatments would be required to clarify this question.

#### Section 4

#### SUMMARY

Recovery of tensile flow stress of four binary aluminum alloys and of the high-purity base aluminum was studied under no-load conditions at temperatures of 80°, 120°, 160°, and 200°C for recovery times up to 1,000 hr. In addition, the effect of a concurrent creep strain on the recovery behavior of the five test materials was studied at the 160°C recovery temperature.

The experimental results indicated that at the three higher recovery temperatures, 120°, 160°, and 200°C, and for the longer recovery times the alloys Al-Mg, Al-Zn, and Al-Cu all experienced a greater degree of recovery than the high-purity base aluminum. Of these three alloys, the Al-Cu alloy clearly exhibited the greatest degree of recovery. The Al-Ag alloy was excluded from the comparison because of an apparent strengthening process during recovery.

All the curves representing the fractional flow-stress recovery versus log recovery time under no-load conditions for the unalloyed aluminum and the Al-Mg, Al-Zn, and Al-Cu alloys exhibited plateaus at the higher recovery temperatures and for the longer recovery times. For a given material, this plateau occurred at increasing values of fractional recovery  $f_r$  for increasing recovery temperatures. After this value was reached in a given case, longer recovery times had no further softening effect. Thus, it appears that a stable recovery structure was reached after sufficient recovery time at a constant recovery temperature. However, during recovery under concurrent creep strain at 160°C, the metastable recovery states previously obtained at both the 160° and the 200°C no-load recovery were readily exceeded, in terms of  $f_r$  values.

All the alloys showed a strong increase in flow-stress recovery during creep strain over that experienced during no-load recovery. The additional amount of recovery

increase during creep as a function of creep strain was about the same for the high-purity aluminum and the Al-Mg, Al-Zn, and Al-Cu alloys. The order of increase of total recovery for the alloys was found to be Al-Mg, Al-Zn, and Al-Cu under the no-load recovery conditions and under a creep strain due to a 1,900-psi stress at 160° C.

Part II

RECOVERY BEHAVIOR OF UNALLOYED ARC-CAST MOLYBDENUM

J. L. Lytton

T. E. Tietz

## Section 5

### INTRODUCTION

The recovery of cold-worked metals is accompanied by changes in the arrangement of the dislocations generated during cold work. In recent years, the use of transmission electron microscopy has allowed direct observation of some of the dislocation configurations formed, such as "tangles," networks, cells, subboundaries, and loops. These observations have recently been reviewed by Darken.<sup>(5)</sup> Accordingly, some understanding has been gained concerning the nature of the dislocation rearrangements involved.

The relationship between recovery and the decrease of mechanical strength, however, has only recently been explored. Previous efforts of the authors were directed toward investigating the decrease of tensile flow stress of aluminum and Al-1% Mg during recovery<sup>(1)</sup> and the effects of concurrent elastic and plastic strain on the flow-stress recovery of aluminum.<sup>(2)</sup> In addition, an investigation of the effect of four different solute additions on the tensile flow-stress recovery of aluminum has been made. Many important metals, however, have the body-centered cubic (BCC) crystal structure; e.g., iron, molybdenum, tungsten, vanadium, columbium, tantalum, and chromium. These metals might be expected to behave differently during recovery from those with other crystal structures for two reasons. First, the previous and present investigations of aluminum and its alloys have shown that tensile flow-stress recovery is strongly affected by foreign atoms in the lattice. In the BCC metals, interstitial impurities are usually present and might be expected to have various effects upon both flow behavior and recovery. For example, heterogeneous yielding might occur during prestraining. The diffusion of these interstitials can also relock dislocations during recovery so that a yield point might be obtained upon restraining (strain aging). Second, some of the BCC metals (e.g., iron, molybdenum, and tungsten) undergo the familiar structure-sensitive ductility transition and exhibit brittle fracture at suitably low temperatures. It is of considerable interest to determine the effects of recovery on the transition temperature of such metals.

The purpose of the present investigation was to extend our knowledge of flow-stress recovery to the BCC metals and study the effects of recovery on the ductile-brittle transition temperature. Unalloyed recrystallized arc-cast molybdenum was chosen as a test material, since it is of significant engineering interest and exhibits a well-defined ductility transition near room temperature. As in the previous studies, the degree of recovery was measured in terms of the decrease of tensile flow stress. Prestraining and restraining were carried out at 150°C to avoid the possibility of brittle fracture.



Section 6  
EXPERIMENTAL PROCEDURE

6.1 TEST MATERIALS

The arc-cast molybdenum sheet used in this investigation was obtained from the Climax Molybdenum Company of Michigan. It was 0.060 in. thick by 10 in. wide and had been cold-worked and stress relieved. The processing schedule of this sheet material, as supplied by Climax Molybdenum Company, is given in Table 4. The analysis supplied for the arc-cast ingot lists the following weight-percent impurities: 0.030 C, 0.0030 Si, < 0.0001 Ni, < 0.002 Fe, < 0.0006 O<sub>2</sub>, < 0.0001 H<sub>2</sub>, and 0.0003 N<sub>2</sub>.

The as-received sheet was sheared at about 400°F into tensile blanks whose long axes lay in the rolling direction. This was accomplished by heating the sheet with an acetylene torch just prior to the shearing operation.

Table 4

PROCESSING SCHEDULE FOR ARC-CAST MOLYBDENUM

Step	Operation
1	Machine 12 in. diameter casting to 10 in. diameter
2	Extrude to 6-1/4 in. diameter
3	Recrystallize billet
4	Forge to 1-1/4 in. thick sheet bar
5	Recrystallize sheet bar at 2150°F
6	Cross-roll to 1/4 in. plate at about 2100°F
7	Recrystallize at 2150°F
8	Roll to 1/8 in. thick at about 2000°F
9	Roll to 0.073 in. thick at about 1700°F
10	Roll to 0.061 in. thick at about 700°F
11	Stress-relieve at 1700°F

A temperature-sensitive 450°F crayon was used to obtain an initial sheet temperature of 450°F prior to shearing. The specimen geometry employed is shown in Fig. 25. The reduced sections were produced by grinding. To remove surface contamination, each specimen was electropolished in 50%  $\text{H}_2\text{SO}_4$  for about 1 min. This treatment resulted in approximately 0.001 in. surface removal.

The machined and electropolished tensile specimens were recrystallized for 1 hr in vacuum at 1200°C and gas-cooled in flowing helium. Under these conditions, the specimens cooled to below 100°C in about 5 min. The resulting grain size was 1,800 grains per square millimeter.

## 6.2 APPARATUS

All flow-stress recovery tensile tests were performed on an Instron testing machine, using a 10,000-lb load cell. Extensometers were used which employed dual LVDT's arranged so that their output was proportional to the distance between gage points, initially 1 in. apart. (These extensometers are shown pictorially in Part I of this report.) The extensometer output was amplified within the Instron so that load-elongation curves were autographically recorded in each test. The resulting least-counts for the tensile curves thus recorded were 10-lb (670 psi) load and 0.002 strain.

All the tensile tests on arc-cast molybdenum were carried out at 150°C in a stirred silicone oil bath, using a strain rate of 0.03 per minute. This temperature was maintained constant to within 0.5°C by means of a mercury thermoregulator.

The effect of recovery treatment on ductile-to-brittle transition temperature was determined for arc-cast molybdenum using a Table Model Instron with a  $\text{CO}_2$ -air vapor mixing chamber which was capable of controlling at temperatures of -100°F to +600°F. Tensile elongation at a strain rate of 0.03 per min was used as a measure of ductility. Elongation was measured by placing two pencil lines normal to the specimen axis 1.5 in. apart in the reduced section. After fracture, the specimens were reassembled and the new distance between markings measured. In the usual manner, the elongation was taken as the change in length divided by the original length. The specimens used

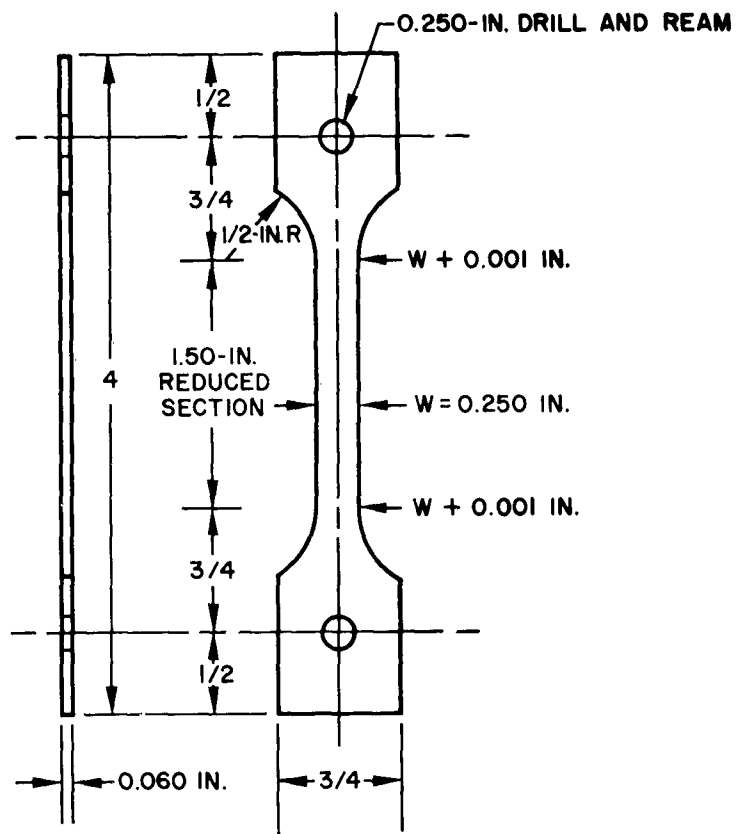


Fig. 25 Molybdenum Tensile Test Specimen Design

for this portion of the investigation were the same as those of Fig. 25, except that the reduced section was machined to a width of 0.100 in.

Recovery treatments were performed on prestrained arc-cast molybdenum specimens at temperatures of 725°C, 801°C, and 901°C. In each case, the specimens were vacuum-encapsulated in a quartz tube to protect them from oxidation. Although dismounting from the extensometer was necessary, the gage point indentations were distinct and the points could be easily repositioned for restraining. The furnaces used were of the resistance-wound type and were controlled by temperature regulators coupled with duration-adjusting type (DAT) units to eliminate temperature overshoot. Recovery temperatures were measured by a thermocouple which was spot-welded to the inside of a close-fitting, 0.005 in. thick stainless steel cylinder, which served as a container for the quartz capsule. This assembly is shown schematically in Fig. 26.

The thermocouple bead was positioned adjacent to the center of the specimen gage section. Recovery treatments were begun by placing this assembly in a furnace which was controlling at the desired temperature and were terminated by removing the assembly and water-quenching until the quartz was cool. The tube was then broken and the specimen water-quenched. The total time between furnace exit and the final specimen quench was about 2 min.

To ascertain the time-temperature path followed by the specimens in reaching each recovery temperature as a function of the temperature of the stainless steel can, a dummy specimen with a thermocouple spot-welded to the center of its gage section was placed in a closed quartz tube and inserted into a stainless steel can to which a thermocouple was attached as in Fig. 26. This assembly was placed in a furnace which was controlling at the desired recovery temperature. The specimen and can temperatures were recorded as a function of time. The following conclusions were drawn from these measurements:

- For each recovery temperature, the specimen achieved steady state in 9 to 10 min.

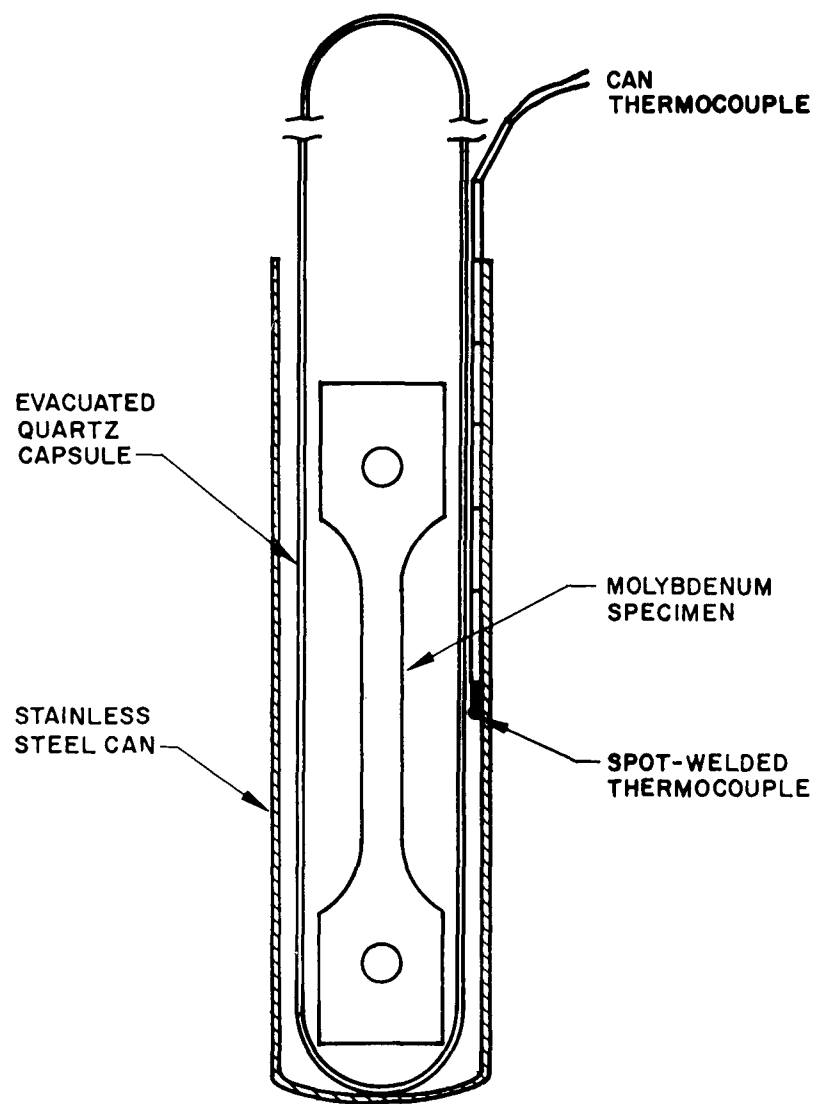


Fig. 26 Schematic View of Stainless Steel Can and Quartz Capsule Assembly

- At steady state, the can temperature was 2.5 to 3°C higher than the specimen temperature. The reported recovery temperatures were accordingly corrected.
- Specimen temperature was held constant during steady state to  $\pm 1^\circ\text{C}$ .
- The effective time at temperature based upon activation energies of 50 to 75 kcal per mole could be taken with sufficient accuracy to be the total time, starting when the can temperature was 5°C below its final steady-state temperature. The difference between this and total time in the recovery furnace was generally about 7 min. In order that this difference not be too large a proportion of the total time, recovery times of less than about 30 min were not employed.
- Recovery temperatures significantly higher than 900°C allowed sufficient recovery during the heat-up period to negate the results for analysis as isothermal recovery.

### 6.3 METHOD OF EVALUATING FLOW-STRESS RECOVERY

In Part I of this report and in the previous study of the recovery behavior of aluminum and Al-1% Mg,<sup>(1)</sup> the fractional decrease in flow stress after 10% true prestrain was used as a recovery parameter. In BCC metals which exhibit the familiar yield point phenomenon, however, such a definition is not possible. A schematic diagram of a stress-strain curve for polycrystalline arc-cast molybdenum before and after recovery is shown in Fig. 27. Initial yielding occurred by nucleation of one or more Lüders bands, usually near the fillets in the reduced section. These bands propagated throughout the gage section and resulted in the Lüders strain,  $\epsilon_L$ , which was generally 0.05 to 0.08. After propagation was complete, uniform strain hardening began. At a true strain of 0.10, the test was stopped and the specimen recovered. Upon restraining, a yield drop was sometimes obtained, although in this investigation no well-defined lower yield stress occurred during restraining. Instead, a minimum stress was obtained, after which the stress immediately began to increase as normal flow occurred. Under these conditions, initial discontinuous yielding masks the initial flow stress which would have caused flow if dislocation locking had not been present. Correspondingly, the yield drops obtained after recovery also mask the initial stress to cause flow in the absence of the dislocation locking which can occur during recovery; i. e., strain aging.



It is possible, however, to define a fractional recovery parameter which will vary from 0 to 1 and will avoid some of these difficulties. Such a parameter is illustrated in Fig. 27. The initial flow curve is projected forward to a true strain of 0.11 and backward to a true strain of 0.01.\* The forward projection becomes the reference flow line for zero recovery; when the initial flow curve is shifted to 0.10 true strain, it becomes a reference for 100% recovery, as shown by the dashed line in Fig. 27. The fractional flow-stress recovery may then be defined as the drop in flow stress,  $\Delta\sigma$ , at some convenient strain divided by the total drop to reach the 100% recovery curve at that strain. For the purposes of this report, a true strain of 0.11 was chosen, since for all the tests this was just beyond any irregularities in the flow curve after recovery. As illustrated in Fig. 27, the fractional flow-stress recovery parameter  $f_r$  is thus defined as:

$$f_r = \frac{\Delta\sigma_{.11}}{\sigma_{.11} - \sigma_{.01}}$$

A similar parameter was employed by Michalak and Paxton<sup>(6)</sup> to represent recovery of zone-melted iron.

The reproducibility of the initial flow curves for arc-cast molybdenum has been good. The flow stress at 10% true strain, for example, was found to be 51,200 psi  $\pm$  2% for all the tests. The value of  $\sigma_{.01}$  from the extrapolation of three nearly identical flow curves was found to be 27,000 psi. This value was used in the calculation of  $f_r$  for all the data reported herein.

The aforementioned technique of encapsulating the prestrained molybdenum specimens in quartz necessitated a time period between prestrain and restrain during which the specimens were at room temperature for 2 to 4 days. To determine whether this produced any appreciable recovery, several control specimens were re-strained without

---

\*The extrapolation to 0.01 true strain was obtained by drawing a straight line through the flow data plotted as log stress versus log strain.



recovery treatment after the glass blower had encapsulated them. The decrease in flow stress for each of these specimens was less than the recorded ink line on the Instron chart. One control specimen was deliberately stored for 2 weeks. The results upon restraining are shown in Fig. 28. It will be noted that an  $f_r$  of no more than 0.01 resulted from vacuum encapsulation or room-temperature storage for periods up to 2 weeks.

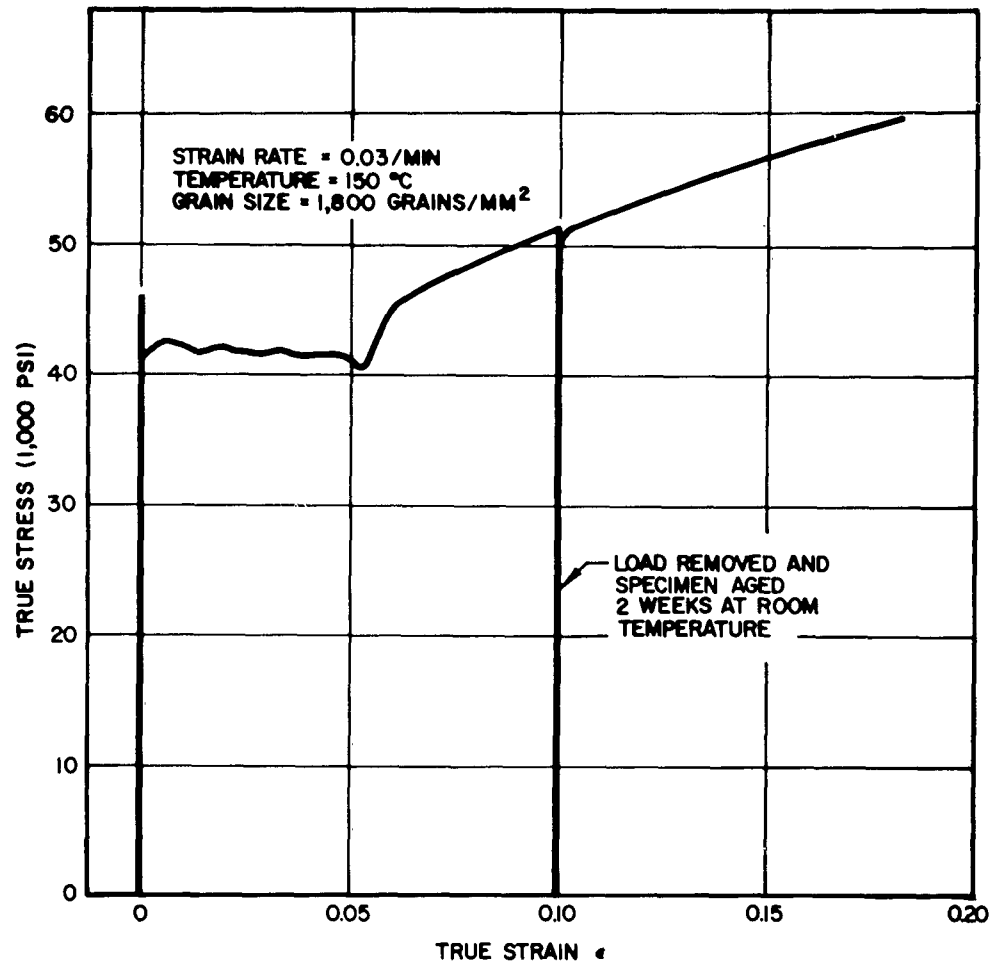


Fig. 28 Effect of Room-Temperature Aging on the Flow Stress at 10% Strain of Recrystallized Arc-Cast Molybdenum

Section 7  
EXPERIMENTAL RESULTS

7.1 STRESS-STRAIN RESULTS

The true stress-true strain curves presented in this section are taken from the auto-graphically recorded curves. Wherever data points are shown, they represent selected values taken from the recorded curves. The stress values for the portions of the initial flow curves which represent discontinuous yielding and flow were calculated using the initial cross-sectional area. The strain values for this region were calculated on the basis of homogeneous strain and are thus artificial until homogeneous straining begins.

One feature of stress-strain curves which exhibit the yield point phenomenon is that the lower yield stress and Lüders strain are dependent upon the number of moving Lüders bands when a constant strain-rate machine is used. It was found in this investigation, however, that the homogeneous flow curve which followed Lüders band propagation was independent of the stress at which the bands propagate (lower yield stress). Three stress-strain curves taken to 0.10 true strain for which three different lower yield stresses were obtained are shown in Fig. 29. The solid line represents homogeneous flow, and the dashed lines at points "A" show the three different lower yield paths followed. The deviation of the three curves during homogeneous flow was less than the width of the solid line shown. The most common lower yield path is the middle one and probably represents the condition for two Lüders bands, one beginning at each fillet.\* The Lüders strain for this condition was about 0.06. In any event, it is clear from Fig. 29 that the homogeneous flow curve for the arc-cast molybdenum of this investigation is independent of the lower yield stress and the Lüders strain.

---

\*Several interrupted tests, for which the Lüders bands were observed, showed the generation of two bands, one at each fillet.

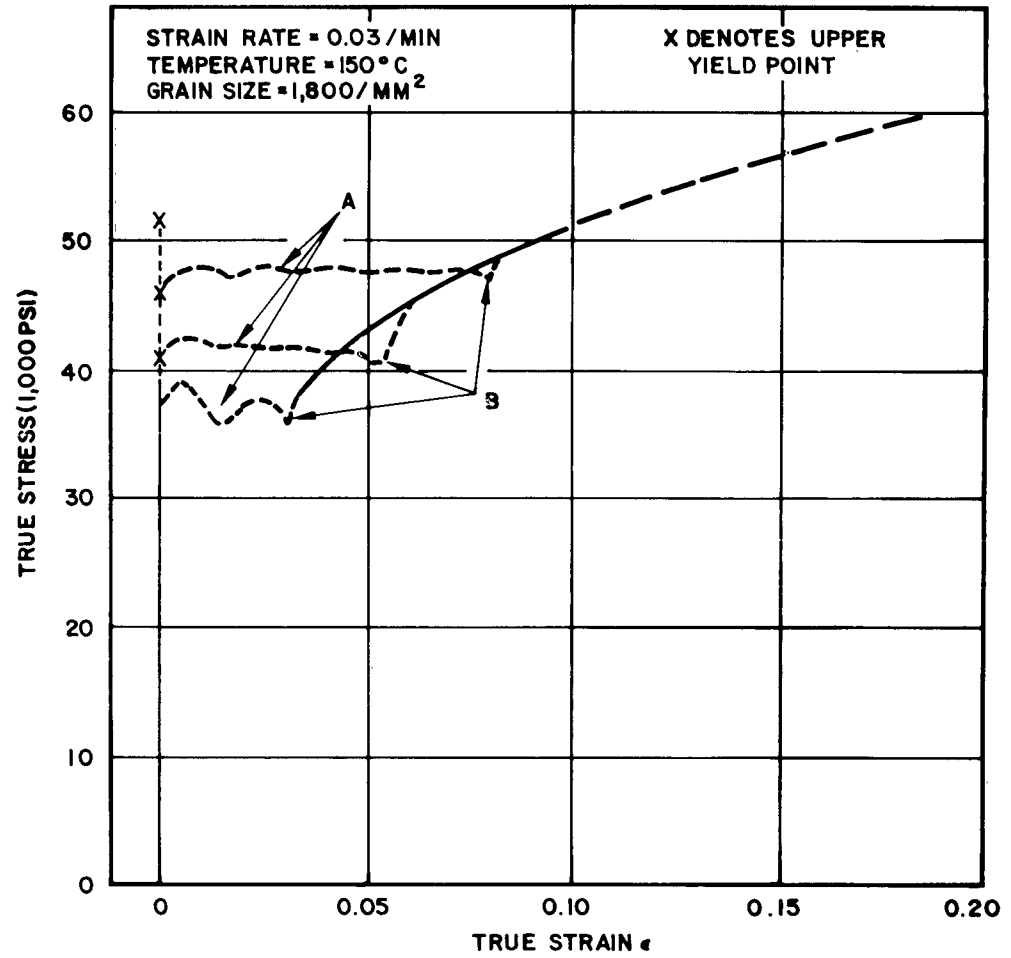


Fig. 29 Stress-Strain Curves for Recrystallized Arc-Cast Molybdenum Showing Various Lower Yield Effects

Another point requiring explanation in Fig. 29 is the "dip" in the curves at points "B" just prior to homogeneous flow. Several tests were conducted at 150°C and were periodically interrupted and observed so that the course of movement of the Lüders fronts could be examined. A typical sequence as two Lüders fronts were observed to come together is schematically illustrated in Fig. 30. As the fronts approached each other, as in Fig. 30a, a definite "kink" was present so that the undeformed section made an angle of 2 deg 7 min with the deformed sections when the fronts were about 1/4 in. apart. The angle of the Lüders fronts tended to stabilize at about 55 deg to the tensile axis in close agreement with the 55- to 60-deg values obtained by Miklowitz<sup>(7)</sup> for flat sheets of silicon steel. As the two fronts came together, they accelerated and formed only one line, as in Fig. 30b. This sudden movement caused the stress to drop suddenly below that required to initiate uniform straining as dictated by the solid curve of Fig. 29. The stress thus must rise steeply to achieve this value before homogeneous flow can begin. During this steep rise, the single Lüders front line illustrated in Fig. 30b was found to disappear.

## 7.2 FLOW-STRESS RECOVERY OF ARC-CAST MOLYBDENUM

The effect of recovery at 725°, 801° and 901°C on the stress-strain behavior of recrystallized arc-cast molybdenum is shown in Figs. 31, 32, and 33. The dashed lines represent an extension of the prestrain curve drawn with the aid of actual test curves taken beyond 0.10 true strain without recovery treatment. The flow curves after recovery are offset so as to avoid confusion. Two points may be noted from Figs. 31, 32, and 33:

- Immediately upon restraining at 150°C after recovery, each curve exhibits either a yield drop as in Fig. 31 for 0.5 hr or an inflection so that the apparent rate of strain hardening increases with increasing strain as for 115 hr in Fig. 31. This behavior is typical of all the curves shown, and it will be noted that the yield drop decreases with increasing recovery time at a given temperature for the temperatures reported herein.

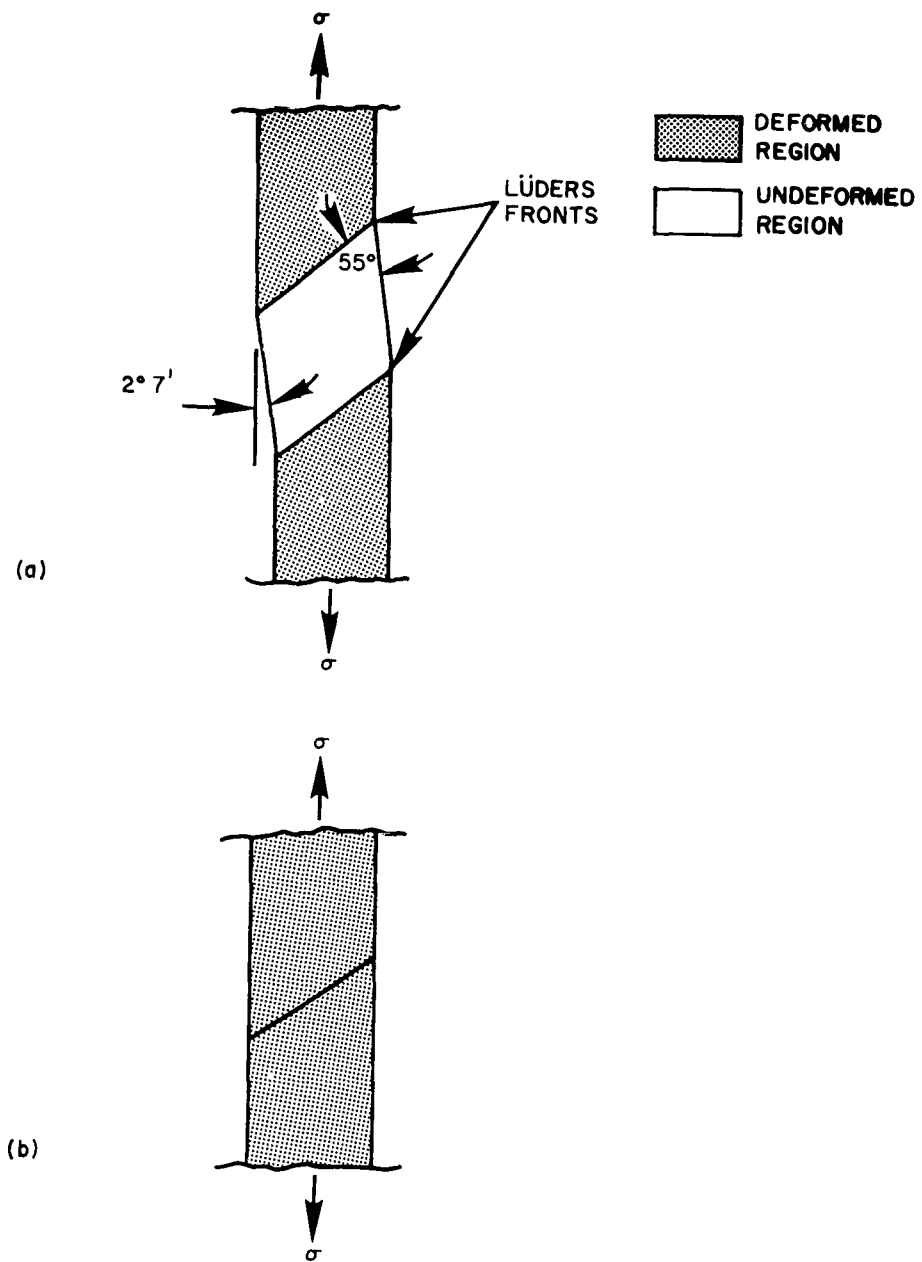


Fig. 30 Schematic Illustration of the Joining of Two Lüders Bands During Tensile Straining of Arc-Cast Molybdenum

- After the initial "anomalous" yield drop or inflection, apparently normal strain-hardening occurs. Reference to the dashed lines of Figs. 31 and 32, however, shows that the flow stress eventually exceeds that for zero recovery for the 0.5 hr recovery times at 725° and 801°C. This was also true for the recovery times of 2 hr and 6 hr at 725°C and 2.5 hr at 801°C. The remaining curves either join the projected curve for zero recovery or fall below it, as in Fig. 33.

The effect of recovery time on the fractional flow-stress recovery  $f_r$ , as previously defined, is shown in Fig. 34. In the early stages of recovery, the curves are seen to be slightly concave downward. At an  $f_r$  of about 0.10, they inflect so that below an  $f_r$  of about 0.15 they are concave upward. If the assumption of equal recovered states at equal values of  $f_r$  is valid, the activation energies shown in Fig. 34 are obtained. It will be noted that the values vary from 32,600 to 82,500 calories per mole and seem to increase with increasing recovery and increasing temperature. Further mention of this point will be made later.

To check the possible validity of the assumption of equal recovered states at equal values of  $f_r$ , additional recovery tests were run on three specimens which had essentially identical prestrain curves. These specimens were given recovery treatments which would produce about equal values of  $f_r$  in accordance with the dashed line of Fig. 34; namely, 100 hr at 725°C, 18 hr at 801°C, and 0.93 hr at 901°C. If truly identical recovered states were developed, it would be expected that the stress-strain curves after recovery would superimpose. The stress-strain results are shown in Fig. 35. Superposition is obtained for strains past about 0.105, but it will be noted that the yield anomalies upon initial flow after recovery do not superimpose. It appears that beyond the initial yielding after recovery the assumption of equivalent recovered states at equal values of  $f_r$ , as defined in Fig. 27, is valid. Further discussion of this point will be made later.

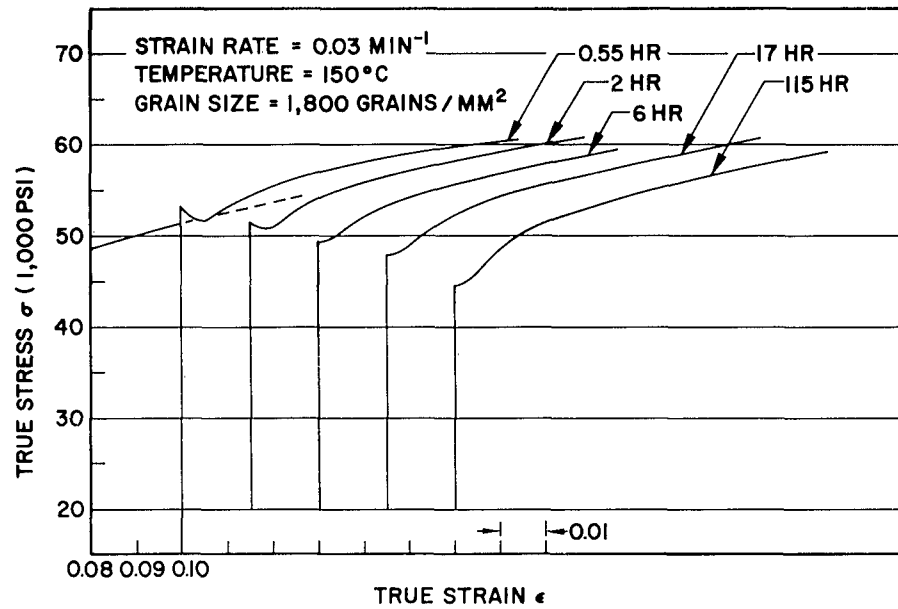


Fig. 31 Effect of Recovery Time at  $725^{\circ}\text{C}$  After 10% Prestrain on the Flow Behavior of Recrystallized Arc-Cast Molybdenum

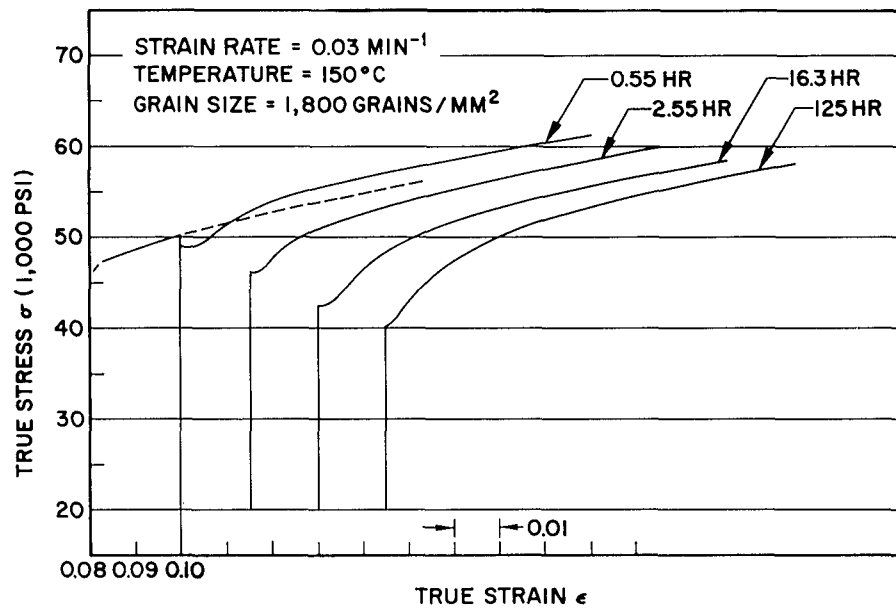


Fig. 32 Effect of Recovery Time at  $801^{\circ}\text{C}$  After 10% Prestrain on the Flow Behavior of Recrystallized Arc-Cast Molybdenum

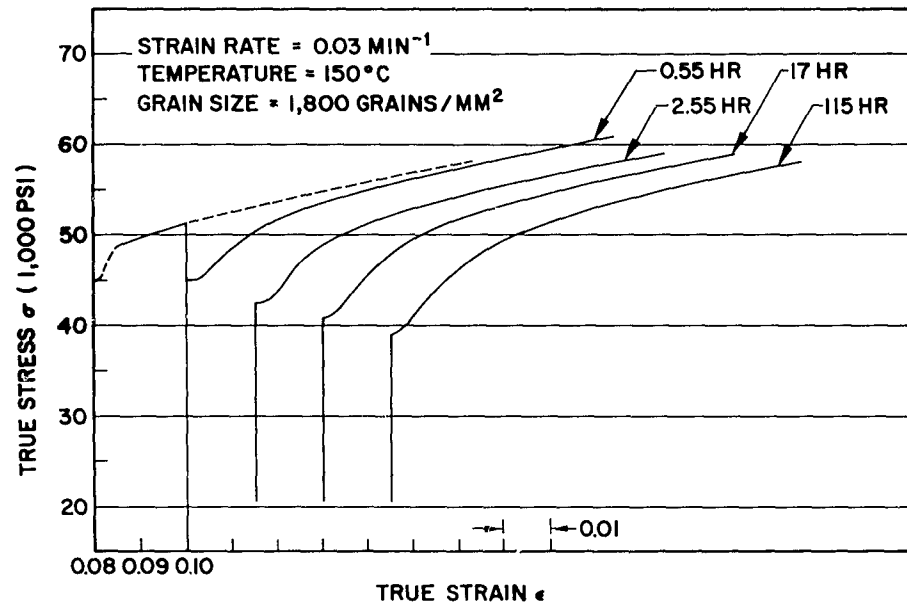


Fig. 33 Effect of Recovery Time at  $901^{\circ}\text{C}$  After 10% Prestrain on the Flow Behavior of Recrystallized Arc-Cast Molybdenum



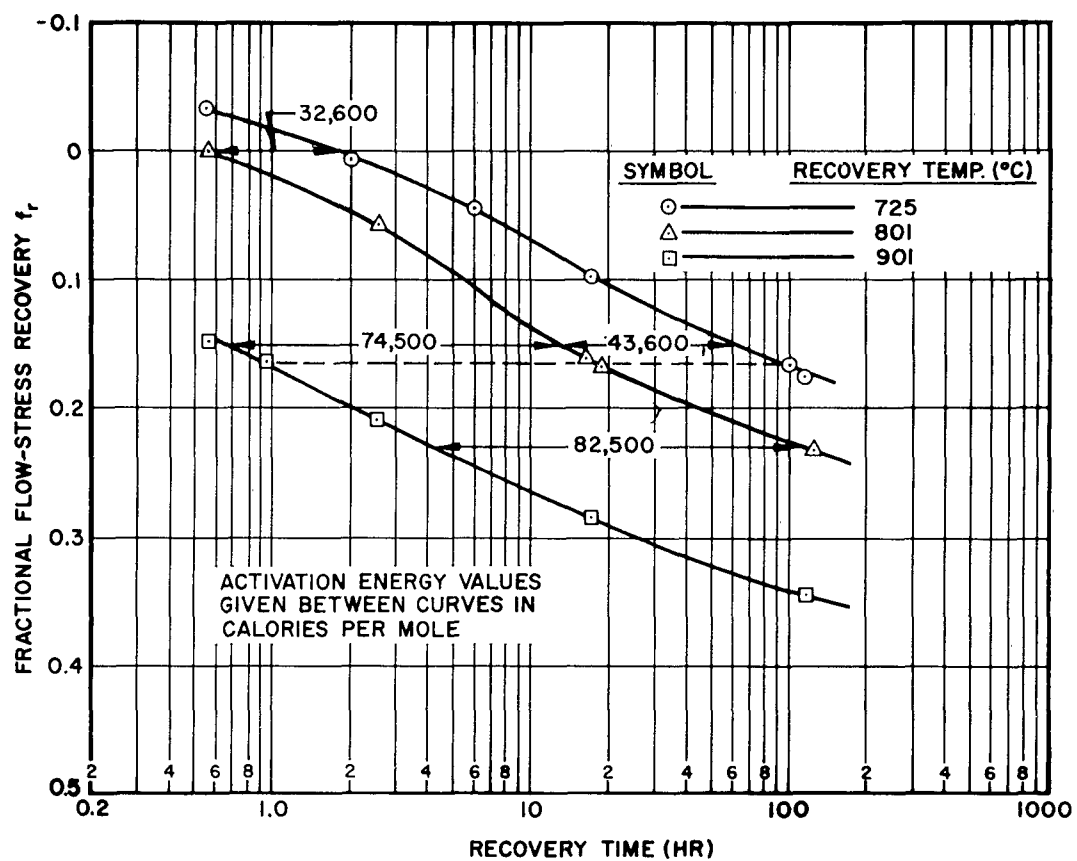


Fig. 34 Effect of Recovery Time on the Fractional Flow-Stress Recovery of Recrystallized Arc-Cast Molybdenum for Three Recovery Temperatures

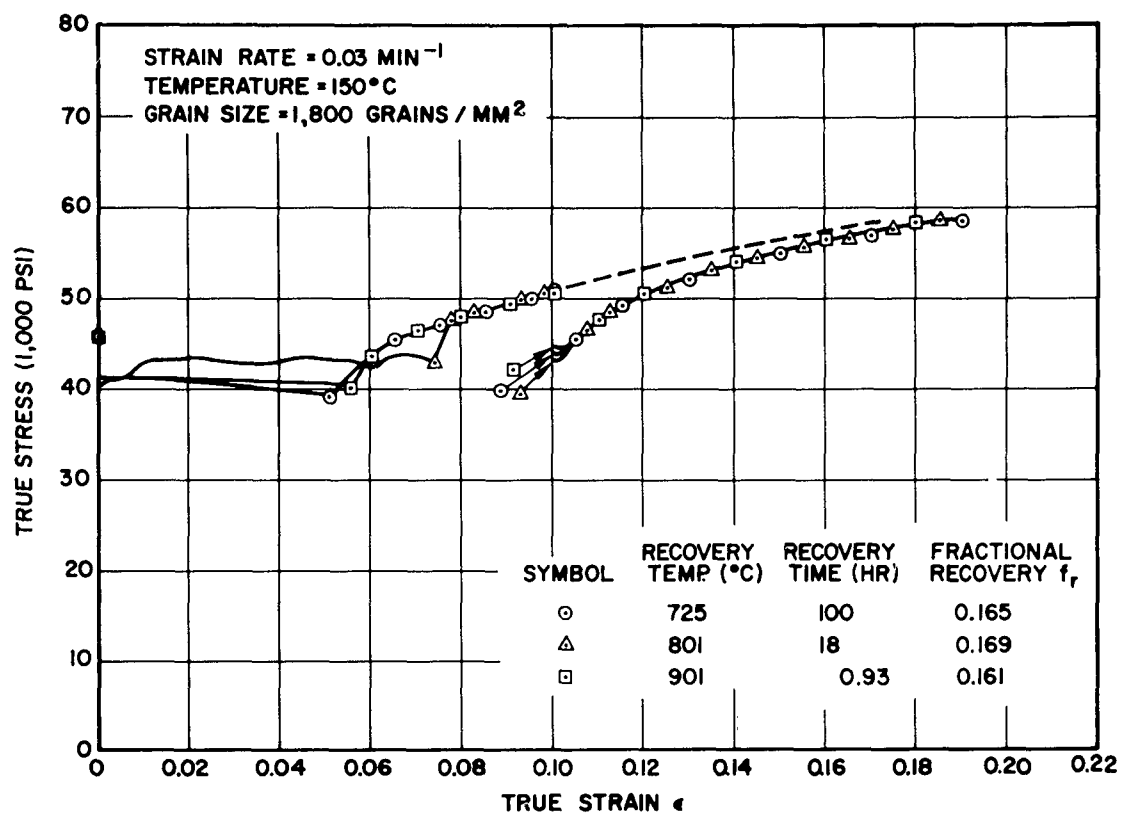


Fig. 35 Stress-Strain Curves for Three Arc-Cast Molybdenum Specimens With Equal Values of Fractional Flow-Stress Recovery

### 7.3 EFFECT OF RECOVERY ON THE DUCTILITY OF ARC-CAST MOLYBDENUM

As a preliminary investigation, the effect of 10% prestrain at 150°C and recovery treatment for 1 hr and 100 hr at 801°C on the ductile-to-brittle transition temperature of recrystallized arc-cast molybdenum was determined using tensile elongation to fracture. The results are shown in Fig. 36, which presents the elongation for the recrystallized, 10% prestrained, and 10% prestrained and recovered molybdenum specimens as a function of test temperature. Three points should be noted from Fig. 36:

- The prestrain treatment of 10% shifted the transition temperature from 10°C to about -22°C. The elongation of the prestrained molybdenum in the ductile range was 25%. This was less than for the recrystallized material in the ductile temperature range because of the prestrain which was not included in the total elongation of the prestrained samples. Thus, the prestrain curve should be 10% below the recrystallized curve at a test temperature of 150°C.
- The effect of recovery treatment at 801°C for 1 hr and 100 hr on the transition temperature was nearly the same; i.e., the transition temperature was shifted to about -5°C. Recovery for 100 hr did appear to shift this temperature slightly more than 1 hr, but the majority of the effect was obtained within the first hour.
- One hour of recovery at 801°C had little effect upon the elongation above the transition temperature, but 100-hr recovery increased the elongation to about 34%, only a few percent below that of the recrystallized molybdenum.

Because of the preliminary nature of these results, no detailed discussion of these data will be given. Two definite conclusions, however, may be drawn. First, the shift of transition temperature due to 10% prestrain and subsequent recovery is sufficient to allow study of the effects of recovery on the ductile-brittle behavior of molybdenum. Second, the effect of even short-time recovery at 801°C is to shift the transition temperature of the prestrained material back toward that of the recrystallized material.

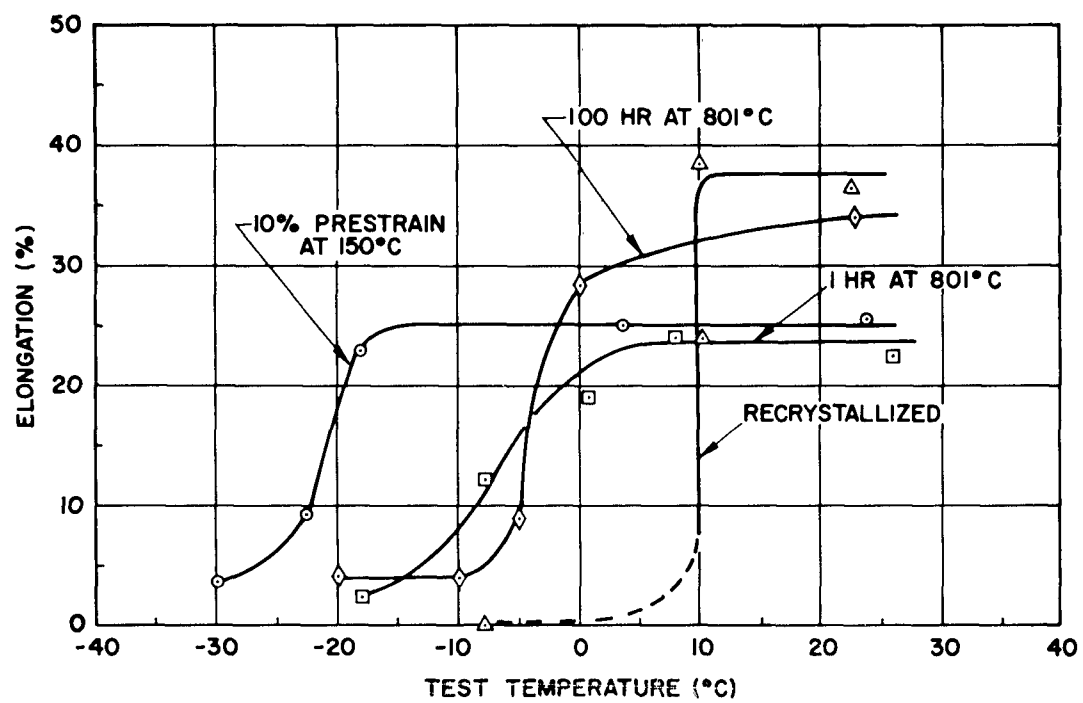


Fig. 36 Effect of Prestrain and Recovery Treatment on the Elongation to Fracture of Recrystallized Arc-Cast Molybdenum

## Section 8

### DISCUSSION

#### 8.1 STRAIN-AGING EFFECTS

The yield drop which was observed to occur upon restraining of molybdenum after recovery was undoubtedly the result of "strain aging" caused by interstitial impurities which diffused to dislocations during the recovery treatment, as described by Cottrell and Bilby.<sup>(8)</sup> Strain-aging experiments have been conducted on arc-cast molybdenum by Brock,<sup>(9)</sup> who measured the rate of yield point return upon heating of prestrained samples. Brock found that the activation energy for strain-aging between 575°C and 700°C was 36,300 calories per mole. This value is in good agreement with the value for diffusion of carbon in molybdenum of 33,400 calories per mole, which was reported by Sansonov and Latisheba.<sup>(10)</sup> This, combined with the fact that carbon is the major interstitial impurity in arc-cast molybdenum, suggests that interstitial carbon is responsible for the strain-aging observed.

Brock also found that at higher strains (above about 5%) recovery effects tended to exceed the strengthening effects of strain aging, so that overall weakening occurred. Thus, the higher temperatures and 10% prestrain employed in this study would be expected to produce overaging; i. e., a decreasing yield stress with increasing recovery time. Reference to Figs. 31, 32, and 33 shows that such is the case. It may be noted, however, that the activation energy shown in Fig. 34 at "zero" recovery is 32,600 calories per mole, a value in close agreement with the aforementioned value for the diffusion of carbon in molybdenum. As annealing proceeds, recovery effects predominate; the activation energy increases as the yield drop diminishes and virtually disappears. These activation energies will be discussed briefly later.

Reference to Figs. 31 and 32 also shows that the transition to "normal" strain-hardening after a yield drop is smooth and does not contain a flat portion indicative of Lüders-type

heterogeneous yielding. Hahn<sup>(11)</sup> has recently developed a model for yielding of BCC metals which proposes that dislocations which are initially locked remain locked and that the yield point is a result of the rapid multiplication and acceleration of dislocations in response to the high applied stress. Hahn's analysis shows that homogeneous yielding under these conditions can lead to a smooth yield drop similar to the drops shown in Figs. 31 and 32. It is quite possible, therefore, that the yield phenomena observed following recovery in this study represent homogeneous yielding. The cause of the decrease in the yield drop with increasing recovery, however, is not easily resolved, since variation of several parameters in Hahn's treatment could account for such changes.

Two further aspects of the strain-aging effects observed during recovery in this study are worthy of note: (1) the yield drop which occurred after recovery decreased with increasing recovery, and (2) the flow stress after yielding for the shorter recovery times exceeded the projected values for zero recovery. The work of various investigators<sup>(12,13)</sup> strongly suggests that microprecipitates can be formed along dislocations in strain-aged steel. Quite possibly the "negative recovery" shown in Fig. 34 for 725°C is the result of the strengthening effect of microprecipitates in the lattice, presumably carbides. Correspondingly, the decrease of the yield drop as recovery increases could be a result of decreased dislocation locking as the matrix becomes depleted of solute carbon as the precipitate is formed.

## 8.2 FLOW-STRESS RECOVERY

Michalak and Paxton<sup>(6)</sup> recently reported the results of an investigation of the recovery of zone-melted iron. These authors employed a recovery parameter much like that defined in Fig. 27. Although they encountered a yield point upon prestraining at -78°C, no yield drop was found upon restraining after recovery. These authors found that the activation energy for recovery increased from about 25,000 to 52,000 calories per mole with increasing recovery. Although they assumed no such effect, their data show a tendency toward increasing activation energy with increasing temperature. Both of these types of variations are evident from the results for molybdenum, as shown in Fig. 34. At an  $f_r$  of 0.15, the activation energy varies from 43,600 to 74,500

calories per mole, depending on the temperature. At an  $f_r$  of 0.23, the activation energy for recovery is 82,500 calories per mole between 801°C and 901°C. It seems evident from the curves of Figs. 31, 32, and 33 that below an  $f_r$  of about 0.15, recovery predominates over any strain-aging effects, and thus the activation energies obtained are indicative of those for recovery.

Some of the possible structural changes which might occur during recovery of BCC metals have been observed using the transmission electron microscope. Brandon and Nutting<sup>(14)</sup> and Hale et al.<sup>(15)</sup> showed that during prestraining of iron, dislocation "tangles" formed into cell walls. Upon annealing, these cell walls tended to rearrange themselves into subboundary networks. Dislocation loops were also observed.<sup>(14,16)</sup> Similar observations have been made by Benson et al.<sup>(16)</sup> for deformed and recovered sintered molybdenum sheet. The results of the previous investigations of aluminum<sup>(1,2)</sup> suggest that subgrain coarsening might also occur. Because of the occurrence of cross-slip,<sup>(17)</sup> dislocation rearrangement would not always require dislocation climb and the accompanying diffusion of vacancies. It might thus be expected that the activation energies for recovery would be less than the energy for self-diffusion. It is interesting to note that the activation energies obtained for flow-stress recovery of molybdenum, iron, and aluminum all appear to bear some relationship to absolute melting temperature. The activation energies of this investigation, those of the previous year's investigation of aluminum,<sup>(1)</sup> and the results of Michalak and Paxton for iron<sup>(6)</sup> are shown in Fig. 37 as a function of absolute melting temperature. The straight line shown for self-diffusion represents a ratio of activation energy to melting point of 38 taken as an average of the values for metals listed by Cottrell.<sup>(18)</sup> The spread of values for recovery in iron and molybdenum each falls below that for self-diffusion. The ranges obtained, however, bear a linear relationship to the melting point, the average energy for flow-stress recovery being about 22 times the melting point. The tendency in both BCC metals is toward higher activation energies with increased recovery and temperature. The value of 23,000 calories per mole previously obtained for aluminum<sup>(1)</sup> is in close agreement with that for iron and molybdenum on the basis of melting point, although no significant variation with either temperature or degree of recovery was detected.

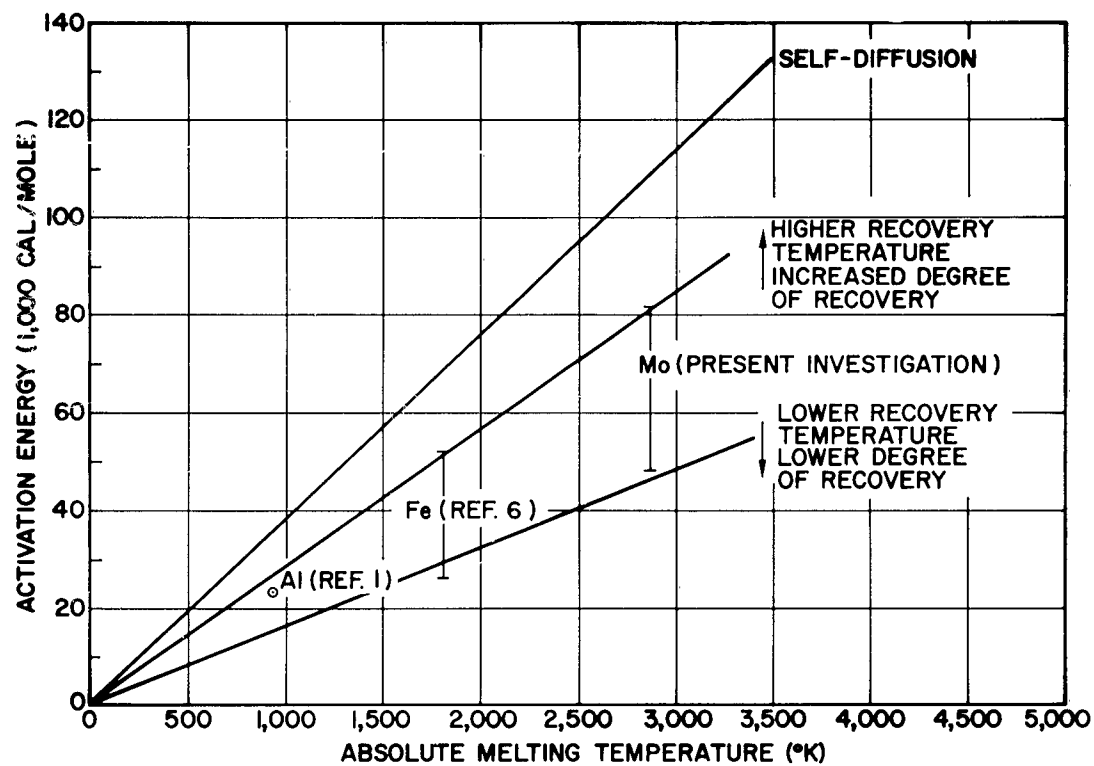


Fig. 37 Effect of Melting Temperature on the Activation Energy for Flow-Stress Recovery of Metals



## Section 9

### SUMMARY

The recovery of flow stress of recrystallized arc-cast molybdenum prestrained 10% at 150°C was studied at temperatures of 725°, 801°, and 901°C. Heterogeneous yielding by Lüders band generation was obtained during prestraining, and the independence of the homogeneous flow curve of the lower yield stress was demonstrated. The yield phenomenon observed after recovery was such that the yield drop diminished and disappeared as recovery proceeded. The initial flow stress in all cases decreased with increased annealing time. A fractional flow-stress recovery parameter  $f_r$  was developed which was found to represent the recovered state aside from initial yield drop effects. Using this parameter, the activation energy for short-time annealing treatments was shown to be equal to 32,600 calories per mole, apparently associated with strain-aging. Above an  $f_r$  value of about 0.15, where recovery was thought to predominate over strain-aging, the activation energy for recovery varied from 43,600 calories per mole to 82,500 calories per mole and was found to increase with increasing degree of recovery and recovery temperature. The activation energies for recovery of aluminum, iron, and molybdenum were shown to be about equal to 22 times the absolute melting temperature.

A 10% prestrain at 150°C was found to shift the ductile-brittle transition temperature of recrystallized arc-cast molybdenum from 10°C to about -22°C. The prestrained molybdenum achieved 24% elongation at room temperature. Recovery annealing for 1 hr at 801°C shifted the transition temperature to about -5°C. Further annealing at 801°C to 100 hr had little additional effect on the transition temperature but increased the ductility at room temperature to 34%.

## REFERENCES

1. T. E. Tietz, C. L. Meyers, and J. L. Lytton, "Recovery of Tensile Flow Stress of Aluminum and Al-1% Mg Alloy," Trans. AIME., Vol. 224, 1962, p. 339\*
2. J. L. Lytton, C. L. Meyers, and T. E. Tietz, "Effect of Elastic and Plastic Strain on the Tensile Flow-Stress Recovery of Aluminum," Trans. AIME. (in press)\*
3. J. E. Dorn, P. Pietrokowsky, and T. E. Tietz, "The Effect of Alloying Elements on the Plastic Properties of Aluminum Alloys," Trans. AIME., Vol. 188, 1950, p. 933
4. A. T. Robinson, T. E. Tietz, and J. E. Dorn, "The Functions of Alloying Elements in the Creep Resistance of Alpha Solid Solutions of Aluminum," Trans. ASM, Vol. 44, 1952, p.896
5. Lawrence S. Darken, "Some Observations on Atoms and Imperfections," Trans. ASM, Vol. 54, 1961, p. 600 (Campbell Memorial Lecture)
6. J. T. Michalak and H. W. Paxton, "Some Recovery Characteristics of Zone-Melted Iron," Trans. AIME, Vol. 221, 1961, p. 850
7. A. Nadai, Theory of Flow and Fracture of Solids, McGraw-Hill, Inc., New York, 1950, p. 318 (quotation from J. Miklowitz)
8. A. H. Cottrell and B. A. Bilby, "Dislocation Theory of Yielding and Strain Aging of Iron," Proc. Phys. Soc., Vol. A62, 1949, p. 49

---

\*These papers present the results given in The Effect of Concurrent Straining and a 1-percent Magnesium Addition on the Recovery Behavior of Aluminum, WADD TR 61-138, Feb 1961 (prepared by Lockheed under USAF Contract No. AF 33(616)-7156, under the direction of the Wright Air Development Division), plus the results of work performed subsequent to publication of WADD TR 61-138.

9. G. W. Brock, "Strain Aging Effects in Arc-Cast Molybdenum," Trans. AIME, Vol. 221, 1961, p. 1055
10. G. V. Sansonov and V. P. Latisheba (Katlinin, Moscow, Institute of Non-Ferrous Metals), Doklady Akad. Nauk S.S.S.R., Vol. 109, 1956, p. 582 (AEC Translation 2949)
11. G. T. Hahn, "A Model for Yielding With Special Reference to the Yield Point Phenomena of Iron and Related BCC Metals," Acta Met., Vol. 10, 1962, p. 727
12. W. R. Thomas and G. M. Leak, "The Strain Aging of Alpha Iron," J. Iron and Steel Inst., Vol. 180, 1955, p. 155
13. D. V. Wilson and B. Russell, "The Contribution of Precipitation to Strain Aging in Low Carbon Steels," Acta Met., Vol. 8, 1960, p. 468
14. D. G. Brandon and J. Nutting, "Dislocations in  $\alpha$ -Iron," J. Iron and Steel Inst., Vol. 196, 1960, p. 160
15. K. F. Hale, W. Carrington, and D. McLean, "Arrangement of Dislocations in Iron," Proc. Roy. Soc., Vol. A259, 1960, p. 203
16. R. Benson, G. Thomas, and J. Washburn, "Dislocation Substructures in Deformed and Recovered Molybdenum," UCRL-9593, Contract No. W-7405-eng-48, Lawrence Radiation Laboratory, Berkeley, Calif., Mar 1961
17. D. G. Brandon and J. Nutting, "The Metallography of Deformed Iron," Acta Met., Vol. 7, 1959, p. 101
18. A. H. Cottrell, Theoretical Structural Metallurgy, Edward Arnold (Publishers), Ltd., 1955, p. 184

Aeronautical Systems Division, Dir./Materials and Processes, Metals and Ceramics Lab, Wright-Patterson AFB, Ohio.  
Rpt Nr ASD-TTR-62-984. RECOVERY BEHAVIOR OF COLD-WORKED METALS. Final report, May 63, 66p incl illus., tables, 18 refs.

Unclassified Report

Recovery of tensile flow stress of four binary aluminum alloys and of the high-purity base aluminum was studied under the no-load conditions at temperatures of 80°, 120°, 160°, and 200°C, and under conditions of creep strain at 160°C, for recovery times up to 1,000 hrs. At the three higher recovery temperatures, 120°, 160°, and 200°C, and for the longer recovery times, the alloys Al-Mg, Al-Zn, and Al-Cu all experienced a greater degree of recovery than the high-purity base aluminum. Of these three alloys, the Al-Cu alloy clearly ex-

( over )

hibited the greater degree of recovery. The Al-Mg alloy was excluded from the comparison because of an apparent strengthening process which occurred during recovery. All the alloys showed a strong increase in flow-stress recovery during creep strain over that experienced during no-load recovery; however, the relative order for recovery for the different alloys did not change. A 10% prestrain shifted the ductile-brittle transition temperature, as indicated by tensile elongation, from 10°C to about -22°C. A 100-hr recovery anneal at 801°C was shown to shift the transition temperature to about -5°C, the major shift occurring during the first hour of recovery.

- i. Aluminum alloys
2. Recovery behavior
- I. AFSC Project 7351.  
Task 735106
- II. Contract AF 33(616)-8346
- III. Lockheed Missiles and Space Co., Sunnyvale, Calif.
- IV. T. E. Tietz, et al
- V. Secondary Rpt No. 2-90-62-1
- VI. Aval fr OTS
- VII. In ASTIA collection

Aeronautical Systems Division, Dir./Materials and Processes, Metals and Ceramics Lab, Wright-Patterson AFB, Ohio.  
Rpt Nr ASD-TTR-62-984. RECOVERY BEHAVIOR OF COLD-WORKED METALS. Final report, May 63, 66p incl illus., tables, 18 refs.

Unclassified Report

Recovery of tensile flow stress of four binary aluminum alloys and of the high-purity base aluminum was studied under the no-load conditions at temperatures of 80°, 120°, 160°, and 200°C, and under conditions of creep strain at 160°C, for recovery times up to 1,000 hrs. At the three higher recovery temperatures, 120°, 160°, and 200°C, and for the longer recovery times, the alloys Al-Mg, Al-Zn, and Al-Cu all experienced a greater degree of recovery than the high-purity base aluminum. Of these three alloys, the Al-Cu alloy clearly ex-

( over )

hibited the greater degree of recovery. The Al-Mg alloy was excluded from the comparison because of an apparent strengthening process which occurred during recovery. All the alloys showed a strong increase in flow-stress recovery during creep strain over that experienced during no-load recovery; however, the relative order for recovery for the different alloys did not change. A 10% prestrain shifted the ductile-brittle transition temperature, as indicated by tensile elongation, from 10°C to about -22°C. A 100-hr recovery anneal at 801°C was shown to shift the transition temperature to about -5°C, the major shift occurring during the first hour of recovery.